Figures and figure supplements

Egr-5 is a post-mitotic regulator of planarian epidermal differentiation

Kimberly C Tu *et al*

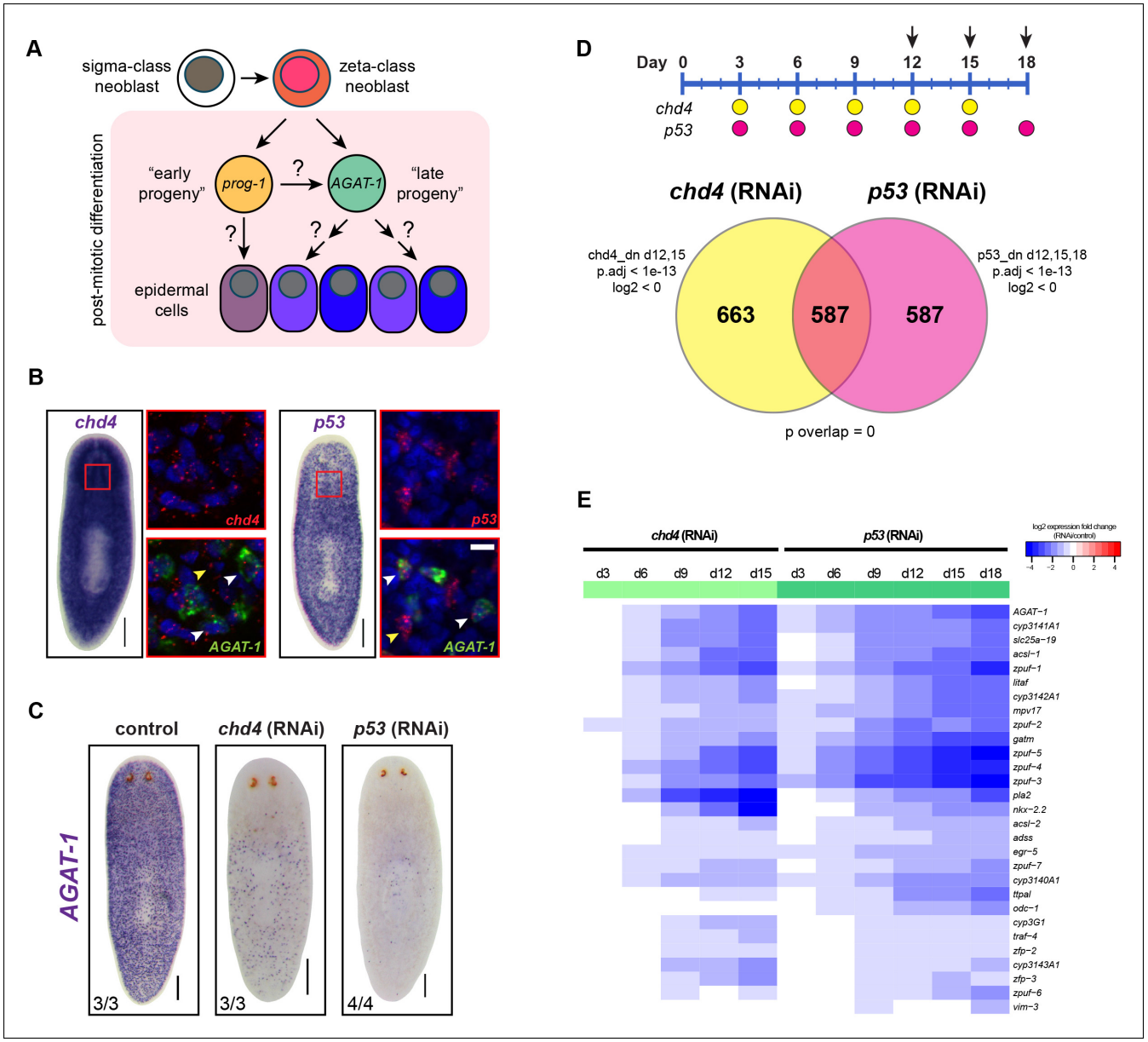

Figure 1. Identification of a common transcriptional down-regulated gene set in *chd4* and *p53* RNAi animals. (**A**) Current model of planarian epidermal lineage specification. Sigma-class neoblasts give rise to zeta-class neoblasts, which in turn generate *prog-1* (early progeny) and *AGAT-1* (late progeny) expressing cells. The precise molecular relationship between these cell types remains unclear, but collectively give rise to an unknown number of epidermal cell types through an unknown number of transitional states. (**B**) Whole-mount in situ (WISH) expression patterns of *chd4* and *p53* in wild-type planaria. Left panels: *chd4* colorimetric WISH and double fluorescent in situ (FISH) of *chd4* (red), *AGAT-1* (green) and DAPI (blue). Right panels: *p53* colorimetric WISH and double FISH of *p53* (red), *AGAT-1* (green) and DAPI (blue). Magnified regions are single confocal planes from boxed regions. White arrowheads highlight cells with co-localized expression of either *chd4* or *p53* and *AGAT-1*. Yellow arrowheads highlight additional mesenchymal cells that do not express *AGAT-1*. Scale bars: 200 μm; 10 μm (zoomed images). (**C**) *chd4*(RNAi) and *p53*(RNAi) result in the loss of *AGAT-1* expressing cells. Representative colorimetric WISH images shown at 3Fd18 of RNAi treatment. Scale bar: 200 μm. (**D**)Venn diagram of genes down-regulated in *chd4* and *p53* RNAi data sets. Timeline of RNAi treatment (Fed d0, d3, d6) and RNA collected for *chd4* (yellow circles) and *p53* RNAi (pink circles). Arrows highlight time points used to identify down-regulated gene set. Criteria used for genes to make the cut-off are shown. dn, down-regulated genes; p.adj, adjusted p-value; log2, fold change of RNAi over control (see Materials and methods). For the *chd4* and *p53* RNAi overlapping data set (587 genes), a hypergeometric distribution and a universe size of 28,668 was used to generate p-value for determining significance of overlap by chance. See also ***Supplementary file 1***. (**E**) Heat map depicting candidate genes that were selected from the *chd4*(RNAi) and *p53*(RNAi) down-

Figure 1. continued on next page

Figure 1. Continued

regulated data sets for further characterization after in situ hybridization screen. log2 fold changes in RNAi expression relative to each control time point are shown.

DOI: http://dx.doi.org/10.7554/eLife.10501.003

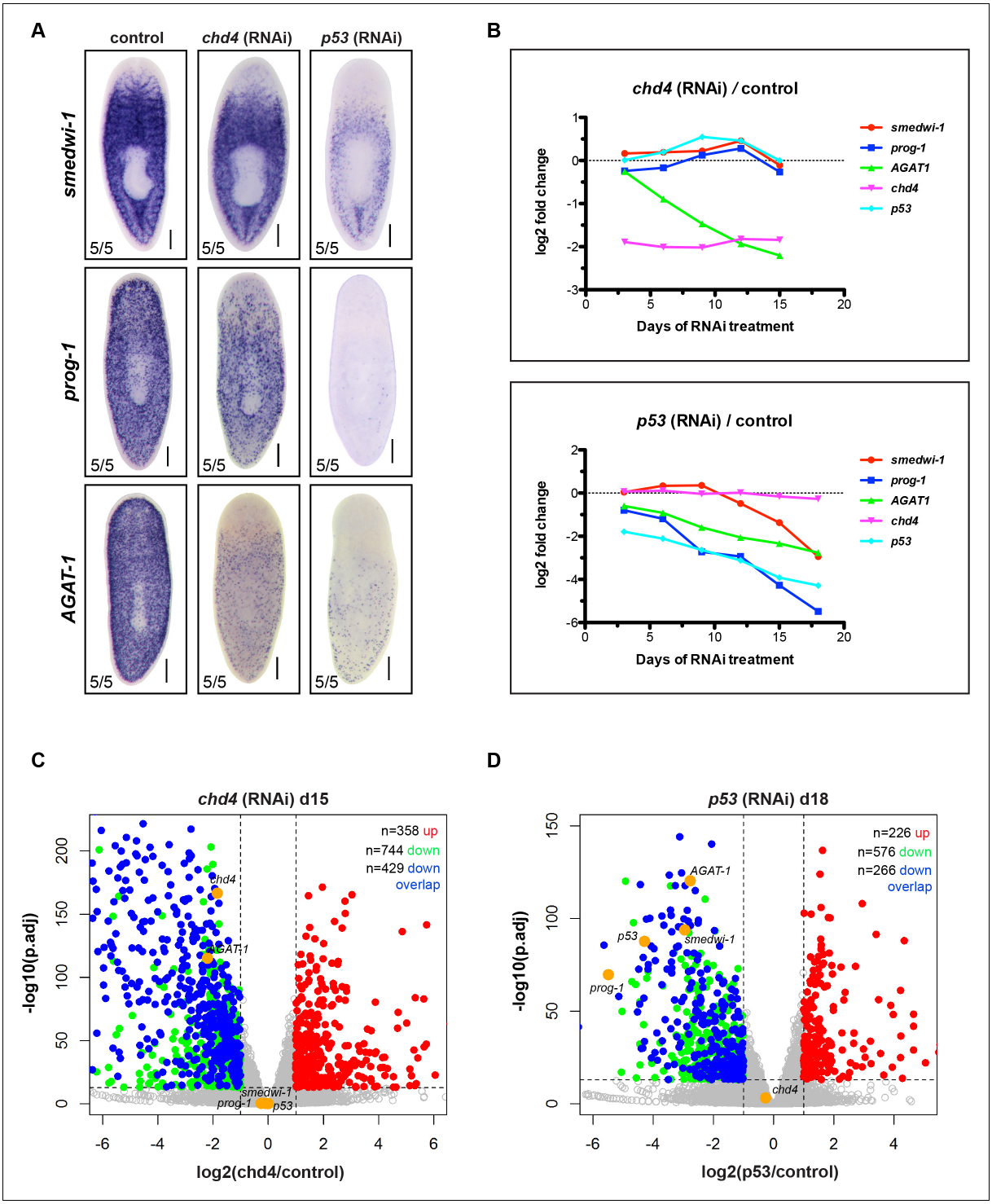

Figure 1—figure supplement 1. RNA-seq validation of control genes in *chd4* and *p53* RNAi animals. (**A**)Colorimetric WISH was performed on control, *chd4* and *p53* RNAi animals for *smedwi-1* (stem cell marker), *prog-1* (early progeny) and *AGAT-1* (late progeny) from the same cohort of worms used for RNA-seq analysis. Representative images of 3Fd15 RNAi worms are shown. Scale bar: 200 μm. (**B**) Plot of log2 ratios of control genes (*smedwi-1*, *prog-1*, *AGAT-1*) and targeted RNAi genes (*chd4* and *p53*) in *chd4*(RNAi) (top panel) and *p53*(RNAi) (bottom panel) time course. For each time point, reads mapping to gene models were counted in *chd4*(RNAi) and *p53*(RNAi) data sets and were then compared to the *unc22*(RNAi) control, and log2 ratios were generated. (**C-D**) Volcano plots illustrating genes significantly down-regulated (green dots; adjusted p-value <1e-13, log2 <-1) and up-regulated

Figure 1—figure supplement 1. continued on next page

Figure 1—figure supplement 1. Continued

(red dots; adjusted p-value <1e-13, log2 >1) at 3Fd15 in *chd4*(RNAi) data set (C) and at d18 in *p53*(RNAi) data set (D). Control genes are highlighted in yellow. Blue dots represent genes from the 587 gene overlap data set (***Figure 1D***) that are also significantly down-regulated in the plotted time points. See also ***Supplementary file 1***. See ***Supplementary file 2*** for up-regulated gene list.

DOI: http://dx.doi.org/10.7554/eLife.10501.004

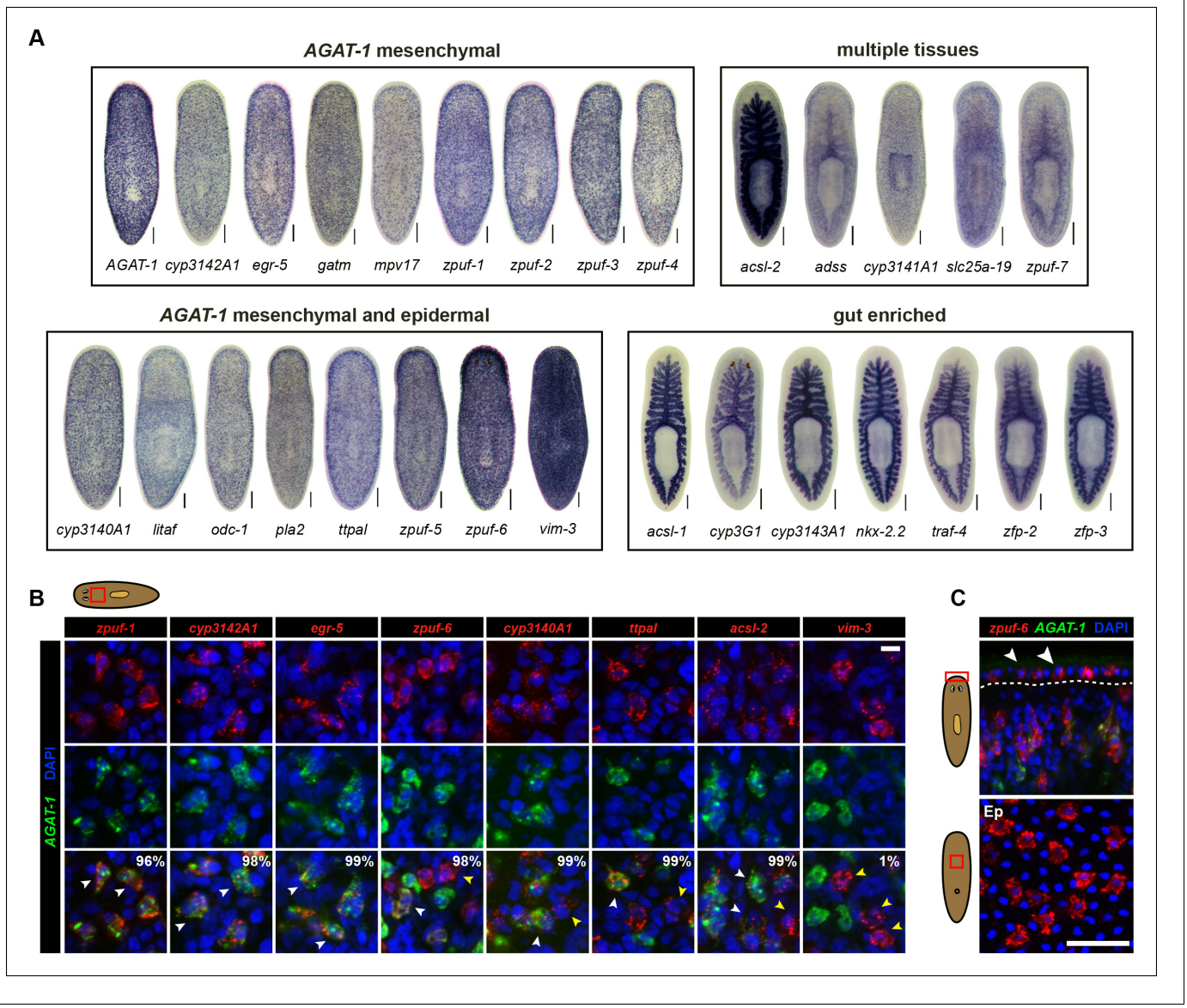

Figure 2. Expression patterns of candidate genes from *chd4*(RNAi) and *p53*(RNAi) data sets. (**A**) WISH expression of representative candidate gene set from ***Figure 1E*** and grouped by expression pattern (see text for details). Scale bars: 200 μm. See also ***Supplementary file 3***. (**B**) Expression pattern of various candidate genes in (**A**), analyzed by double FISH with *AGAT-1*. Images represent single confocal planes from anterior regions. Percentages represent fraction of *AGAT-1*$^{+}$ cells that co-express the candidate gene (~200-400 cells were quantified; low but detectable expression was counted as co-localized). White arrowheads highlight co-localization; yellow arrowheads highlight additional cells that have no detectable *AGAT-1* expression (*AGAT-1*^{neg}). Scale bar: 10 μm. (**C**) Double FISH of *zpuf-6* and *AGAT-1* highlighting *zpuf-6* expression in discrete cells in the planarian epidermis (Top panel, white arrowheads). Bottom panel, ventral epidermal (Ep) view. DapI used for nuclear staining. Scale bar: 50 μm.

DOI: http://dx.doi.org/10.7554/eLife.10501.005

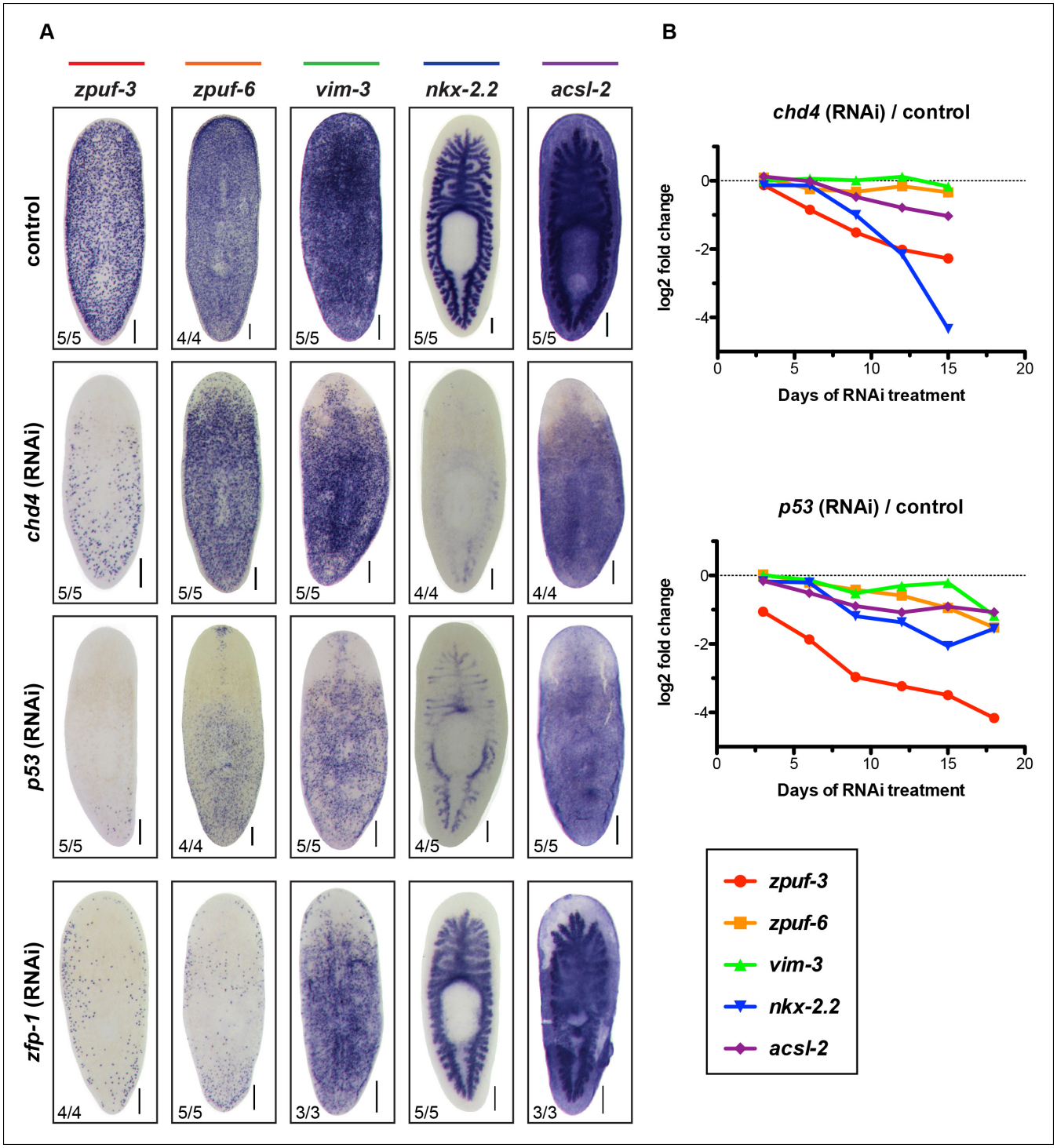

Figure 2—figure supplement 1. Validation of select candidate genes in *chd4*, *p53* and *zfp-1* RNAi conditions by WISH. (**A**) Representative WISH of candidate genes encompassing the full range of expression patterns in control, *chd4* and *p53* RNAi animals fixed at 3Fd21 (For *nkx-2.2*, 3Fd18). Genes expressed in mesenchyme, epidermis and gut are reduced in *chd4* and *p53* RNAi animals. Genes expressed in mesenchyme and epidermis are also reduced in *zfp-1*(RNAi) animals (3Fd21) but gut expression is not affected. Scale bar: 200 μm. (**B**) Plot of log2 ratios of candidate genes from (A) in *chd4* (RNAi) (top panel) and *p53*(RNAi) (bottom panel) RNA-seq time course.

DOI: http://dx.doi.org/10.7554/eLife.10501.006

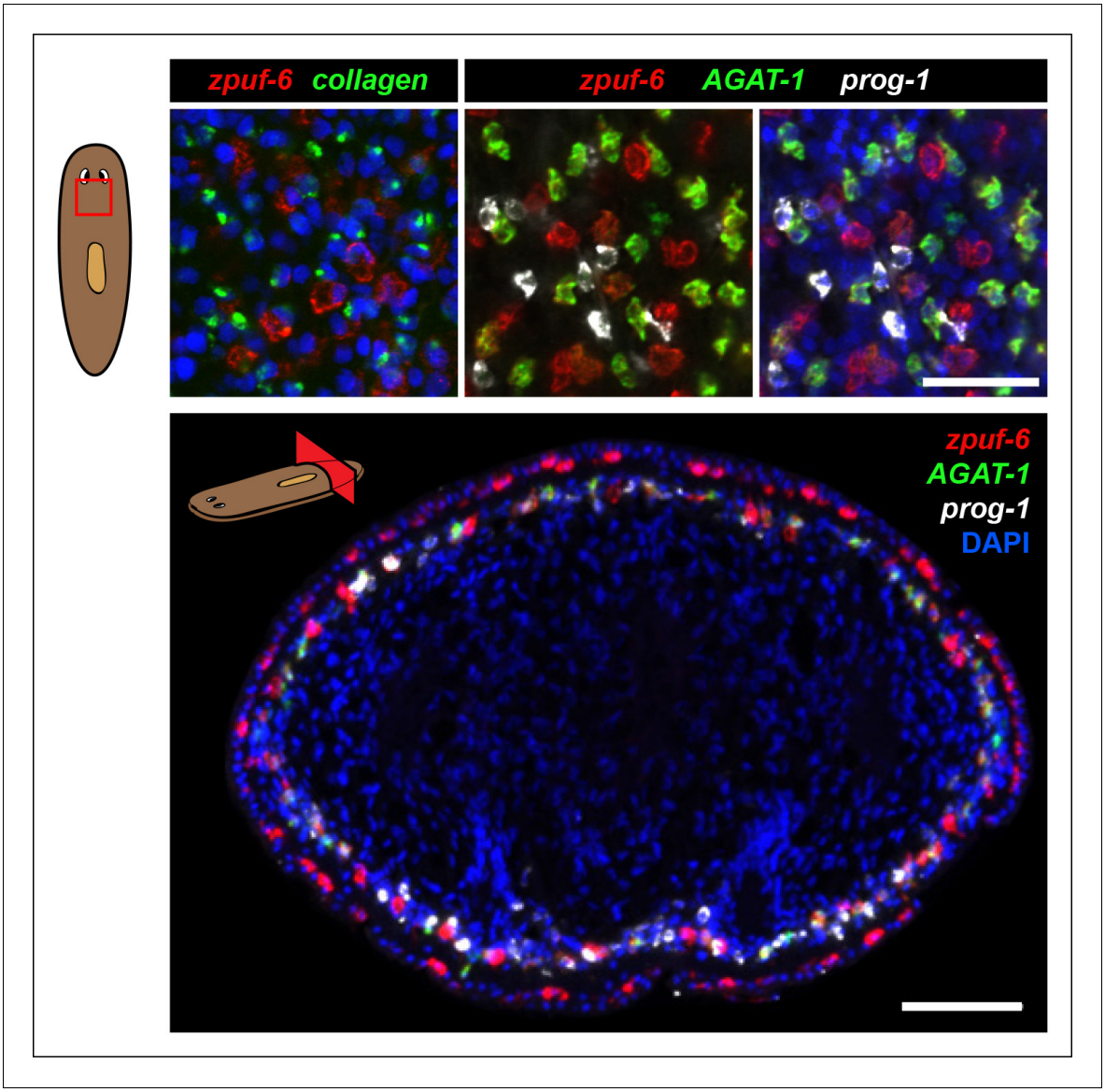

Figure 2—figure supplement 2. Detailed characterization of *zpuf-6* expression pattern by whole-mount FISH. *Zpuf-6* is not expressed in muscle cells or in *prog-1* cells. Top left panel: Double FISH of *zpuf-6* and a muscle marker (*collagen*). Top right panels: Triple FISH of *zpuf-6, AGAT-1* and *prog-1*. Bottom panel: transverse tissue section of triple FISH highlighting the spatial distribution of *zpuf-6, AGAT-1* and *prog-1*. *zpuf-6* is expressed in both sup-epidermal and epidermal layers. All images shown are single confocal planes. Scale bars: 50 μm.

DOI: http://dx.doi.org/10.7554/eLife.10501.007

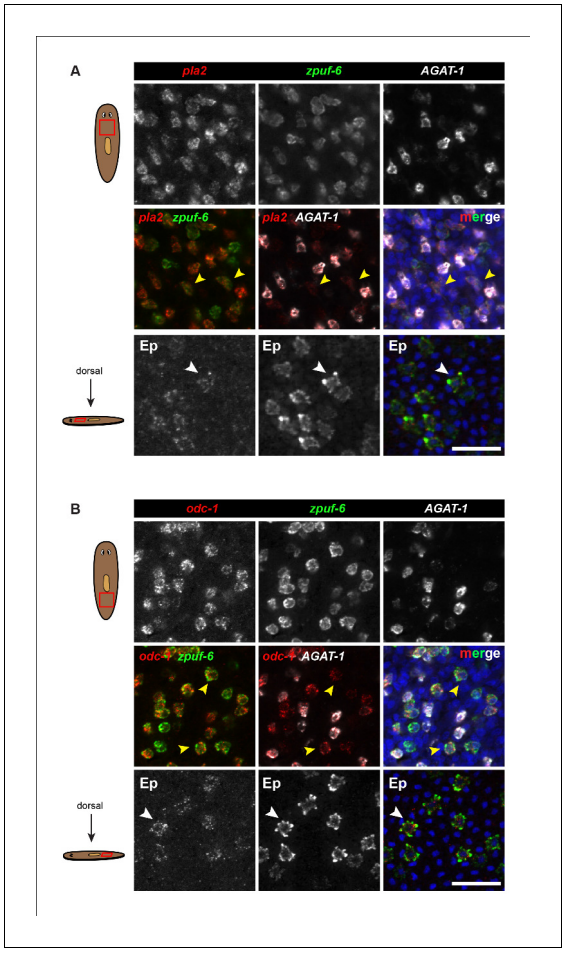

Figure 2—figure supplement 3. Expression of *pla2* and *odc-1* in mesenchyme and epidermis. (**A**) Triple FISH of *pla2, zpuf-6* and *AGAT-1* in the mesenchyme. Top row: single channel of each individual gene. Middle row: Left panel, double FISH of *pla2* and *zpuf-6*. Middle panel, double FISH of *pla2* and *AGAT-1*. Right panel, merge. Yellow arrowheads highlight cells that co-express *pla2* and *zpuf-6* and are *AGAT-1*^{neg}. Bottom row: Double FISH of *pla2* and *zpuf-6* in the epidermis (Ep). White arrowheads highlight co-localization. Scale bars: 50 μm. (**B**) Triple FISH of *odc-1, zpuf-6* and *AGAT-1* in the mesenchyme. Top row: single channel of each individual gene. Middle row: Left panel, double FISH of *odc-1* and *zpuf-6*. Middle panel, double FISH of *odc-1* and *AGAT-1*. Right panel, merge. Yellow arrowheads highlight cells that co-express *odc-1* and *zpuf-6* and are *AGAT-1*^{neg}. Bottom row: Double FISH of *odc-1* and *zpuf-6* in the epidermis. White arrowheads highlight co-localization. Scale bars: 50 μm.
DOI: http://dx.doi.org/10.7554/eLife.10501.008

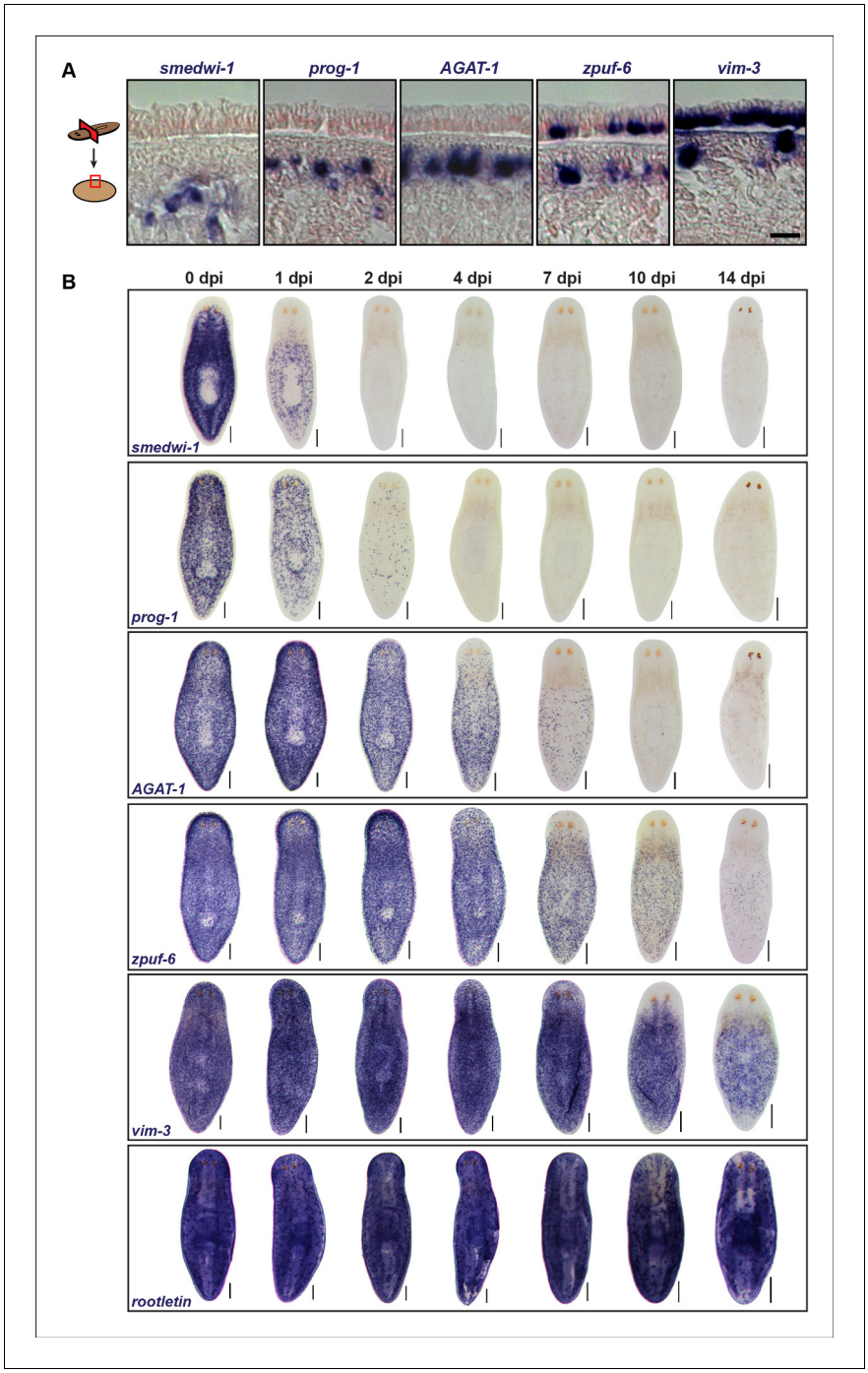

Figure 3. Epidermal progeny markers are expressed in distinct spatiotemporal domains. (**A**) Transverse tissue sections of colorimetric WISH-stained animals expressing putative markers in the epidermal lineage. Sections were counterstained with nuclear fast red. Scale bar: 10 μm. (**B**) Colorimetric WISH of animals after 6000 Rad irradiation exposure for markers of neoblasts (*smedwi-1*), early progeny (*prog-1*), late progeny (*AGAT-1*), and other genes identified in this study (*zpuf-6* and *vim-3*) marking transitions into the epidermis. *Rootletin* marks differentiated cells of the ciliated epidermis as well as protonephridia. Expression patterns of epidermal progeny markers are lost in a ventral-to-dorsal, anterior-to-posterior manner. A representative image from 4–6 worms for each gene and time point are shown. dpi, days post-irradiation. Dorsal views. See ***Figure 3—figure supplement 1*** for close-up ventral views. Scale bars: 200 μm.

DOI: http://dx.doi.org/10.7554/eLife.10501.009

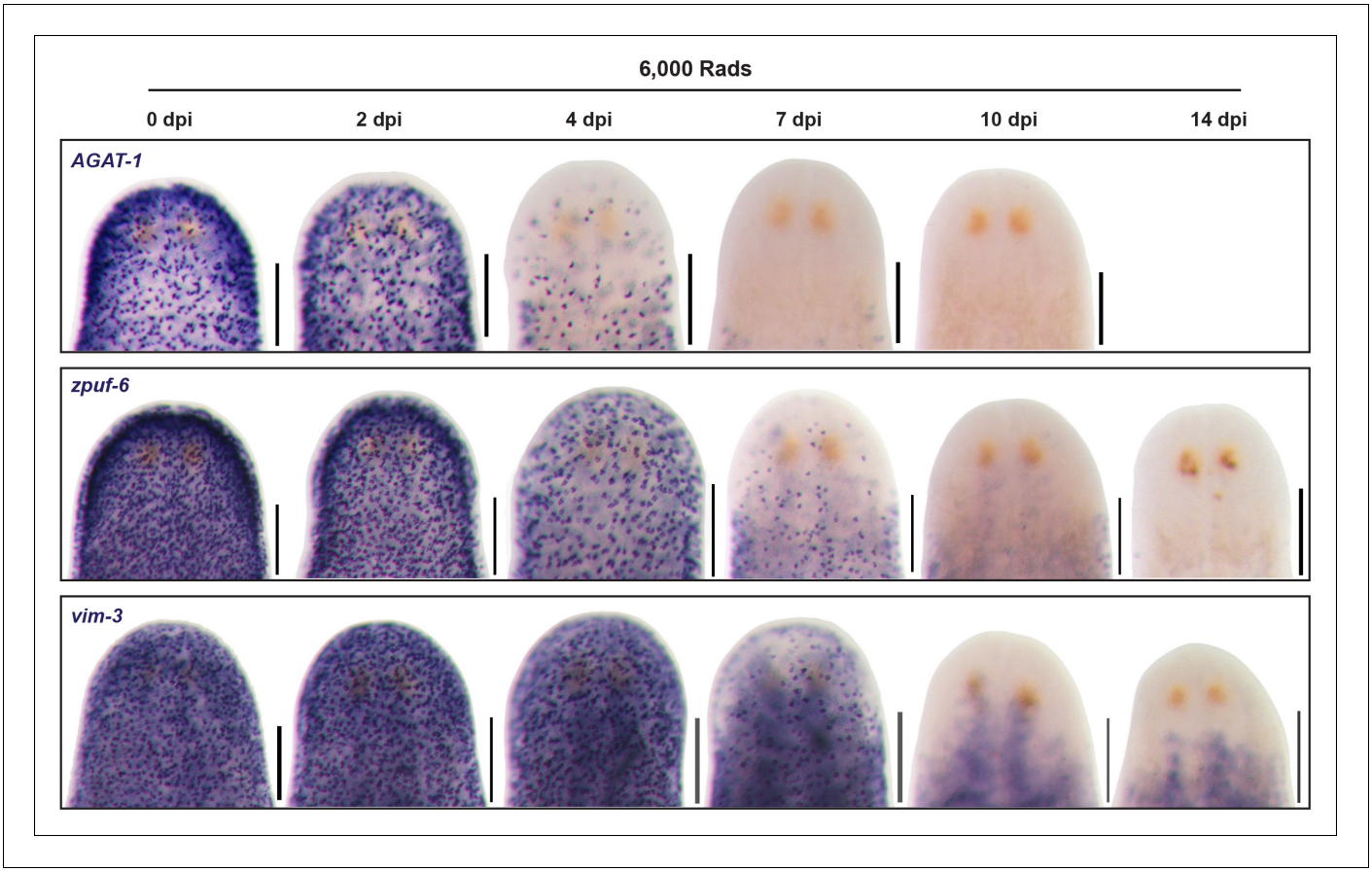

Figure 3—figure supplement 1. Ventral plane sections of epidermal progeny markers after irradiation. Colorimetric WISH of animals after 6,000 Rad irradiation exposure for markers of *AGAT-1*, *zpuf-6* and *vim*-3, highlighting loss of ventral expression prior to loss of dorsal expression. A representative image from 4-6 worms for each gene and time point are shown. dpi, days post-irradiation. Scale bars: 200 μm.
DOI: http://dx.doi.org/10.7554/eLife.10501.010

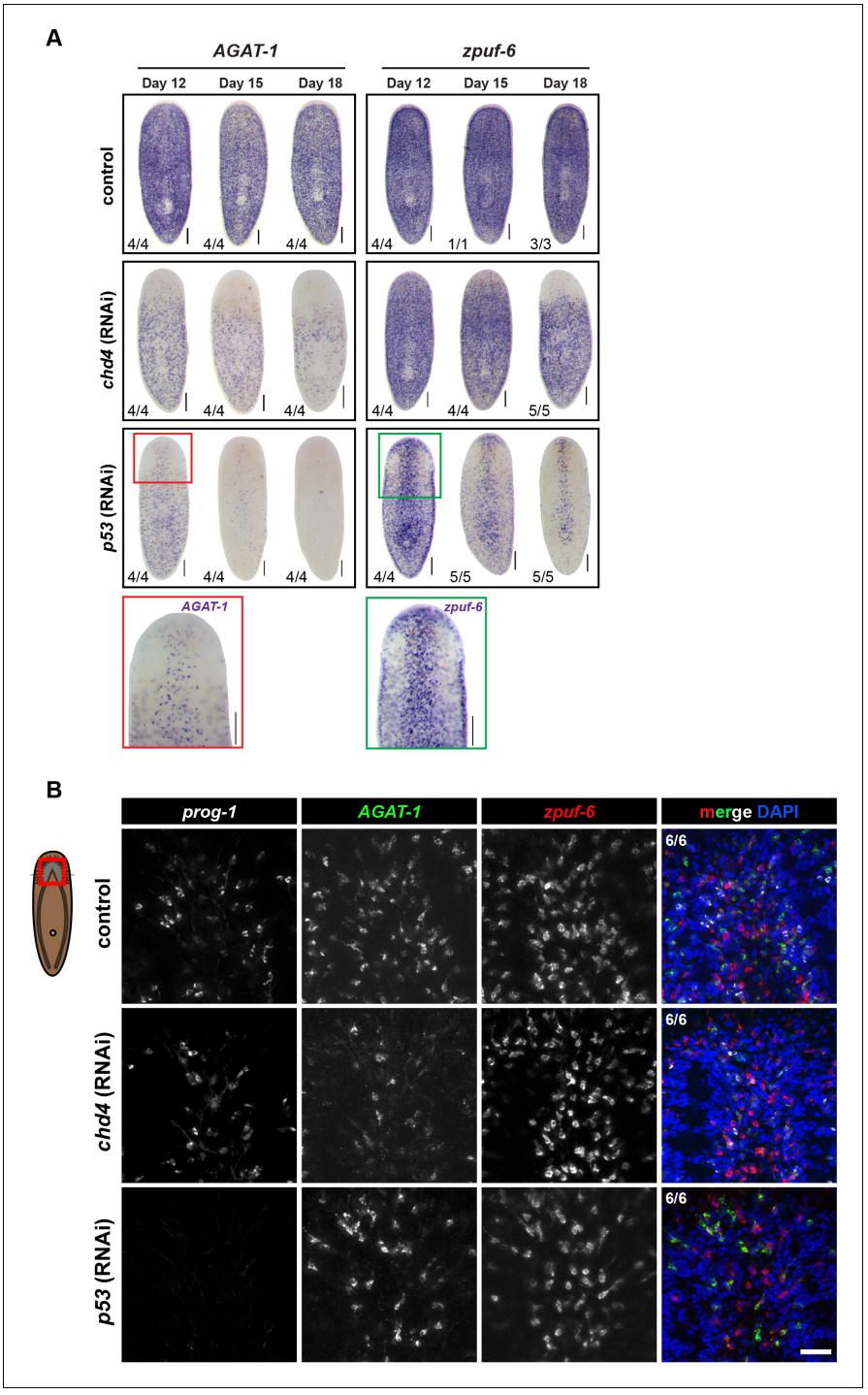

Figure 3—figure supplement 2. Correlated spatial expression patterns of *prog-1*, *AGAT-1* and *zpuf-6*. (**A**) Expression of *AGAT-1* and *zpuf-6* after *chd4* and *p53* RNAi knockdowns. Colorimetric WISH staining is lost in a ventral-to-dorsal, anterior-to-posterior fashion. Expression of markers in *p53*(RNAi) animals display a striped pattern of cells (zoom). Ventral views. Scale bars: 200 μm.(**B**) Triple FISH of *prog-1*, *AGAT-1* and *zpuf-6* at 3Fd12 in control, *chd4* and *p53* RNAi knockdown conditions. The spatial patterns of remaining *AGAT-1* and *zpuf-6* cells are highly correlated. Images shown are single confocal planes of the ventral anterior region. Scale bar: 50 μm.
DOI: http://dx.doi.org/10.7554/eLife.10501.011

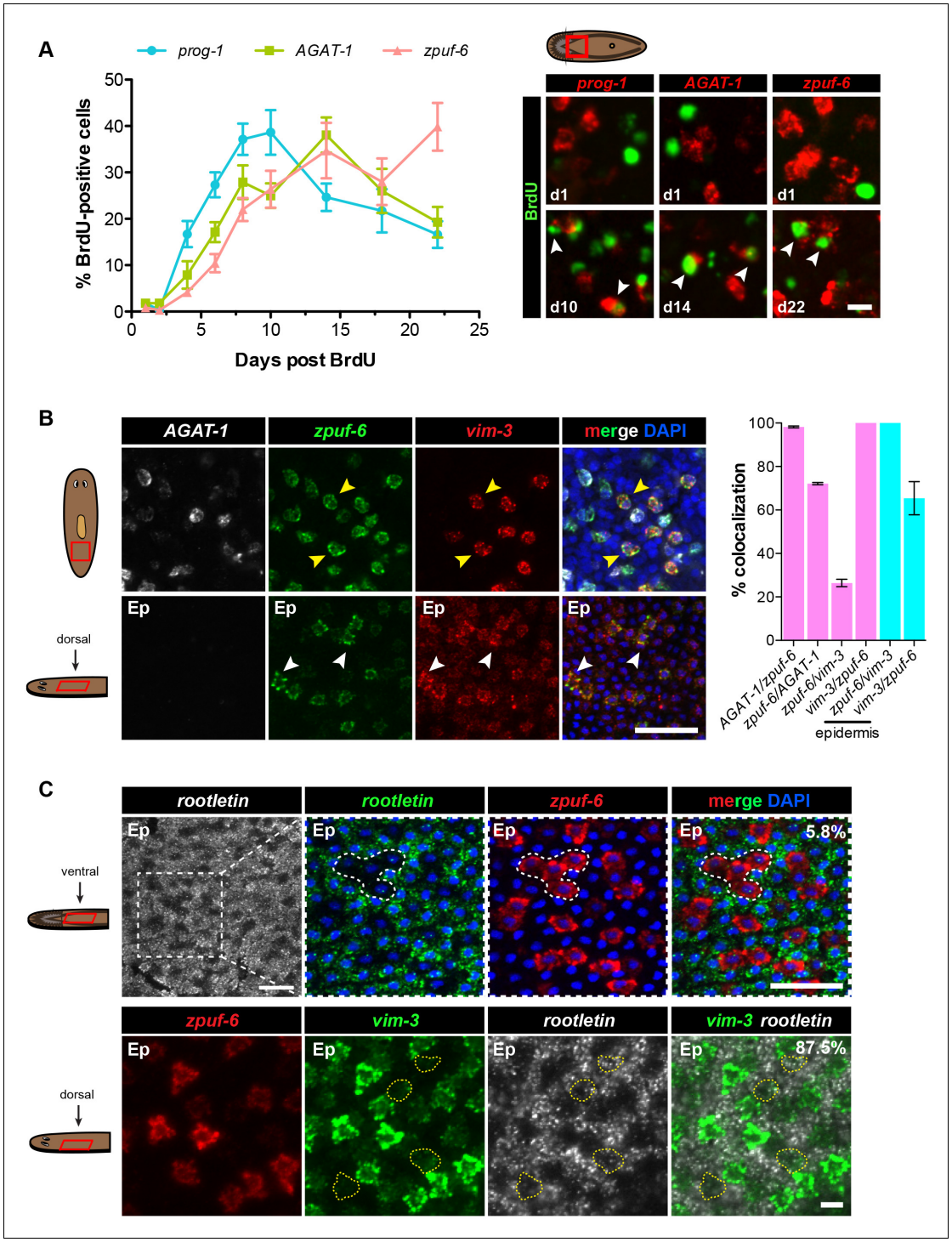

Figure 4. *Zpuf-6*$^{+}$ epidermal cells are not terminally differentiated. (**A**) Turnover dynamics for *prog-1, AGAT-1* and *zpuf-6* expressing cell populations. Animals were soaked with BrdU for 24 hr and chased for the indicated time periods. Quantification of the percentage of *prog-1*$^{+}$, *AGAT-1*$^{+}$ or *zpuf-6*$^{+}$ cells analyzed that are BrdU^{+} are plotted. Error bars: SEM (see Materials and methods). Representative images of BrdU^{+} cells, are maximum intensity projections over 1 cell diameter of a subset of the quantified images, of the minimum and maximum time points for each gene are shown. White arrowheads highlight double-positive cells. Scale bar: 10 μm. (**B**) Lineage relationship between *AGAT-1, zpuf-6* and *vim-3*. Top row: Triple FISH showing overlapping expression between *AGAT-1, zpuf-6* and *vim-3* in the mesenchyme. Yellow arrowheads highlight cells that are *zpuf-6*$^{+}$ *vim3*$^{+}$ *AGAT-1*^{neg}. *AGAT-1* and *vim-3* exhibit little to no co-expression (***Figure 2B***). Bottom row: Dorsal epidermal (Ep) view of *zpuf-6* and *vim-3*. White arrowheads

Figure 4. continued on next page

Figure 4. Continued

highlight cells that co-express *zpuf-6* and *vim-3* but there are additional cells expressing *vim-3*. Images are single confocal planes. Scale bar: 50 μm. Quantifications of the percent colocalizations of combinations of *AGAT-1*, *zpuf-6* and *vim-3* mesenchymal (magenta) and *zpuf-6* and *vim-3* dorsal epidermal cells (cyan) are shown (~200-400 cells were quantified over >3 animals; error bars: SD). *Gene1/gene2* notation signifies percentage of $gene1^+$ cells that are also positive for *gene2* expression. Notable percentages: $zpuf\text{-}6^+/AGAT\text{-}1^+$ (72%), $zpuf\text{-}6^+/vim\text{-}3^+$ (26%). **(C)** *zpuf-6+* epidermal cells express very low levels of *rootletin*. Top row: double FISH of *rootletin* and zpuf-6. 5.8%=percentage of strong *zpuf-6+* epidermal cells that co-express *rootletin* (~300 cells). Scale bars: 50 μm. Bottom row: triple FISH of *zpuf-6*, *vim-3* and *rootletin* in dorsal epidermis. Only overlay of *vim-3* and *rootletin* is shown (far right panel). Yellow-dashed shapes outline cells that express very low levels of *vim-3* that also express *rootletin*. 87.5%=percentage of weak *vim-3+* dorsal epidermal cells that co-express *rootletin* (~200 cells). Images are single confocal planes. Scale bar: 10 μm.

DOI: http://dx.doi.org/10.7554/eLife.10501.012

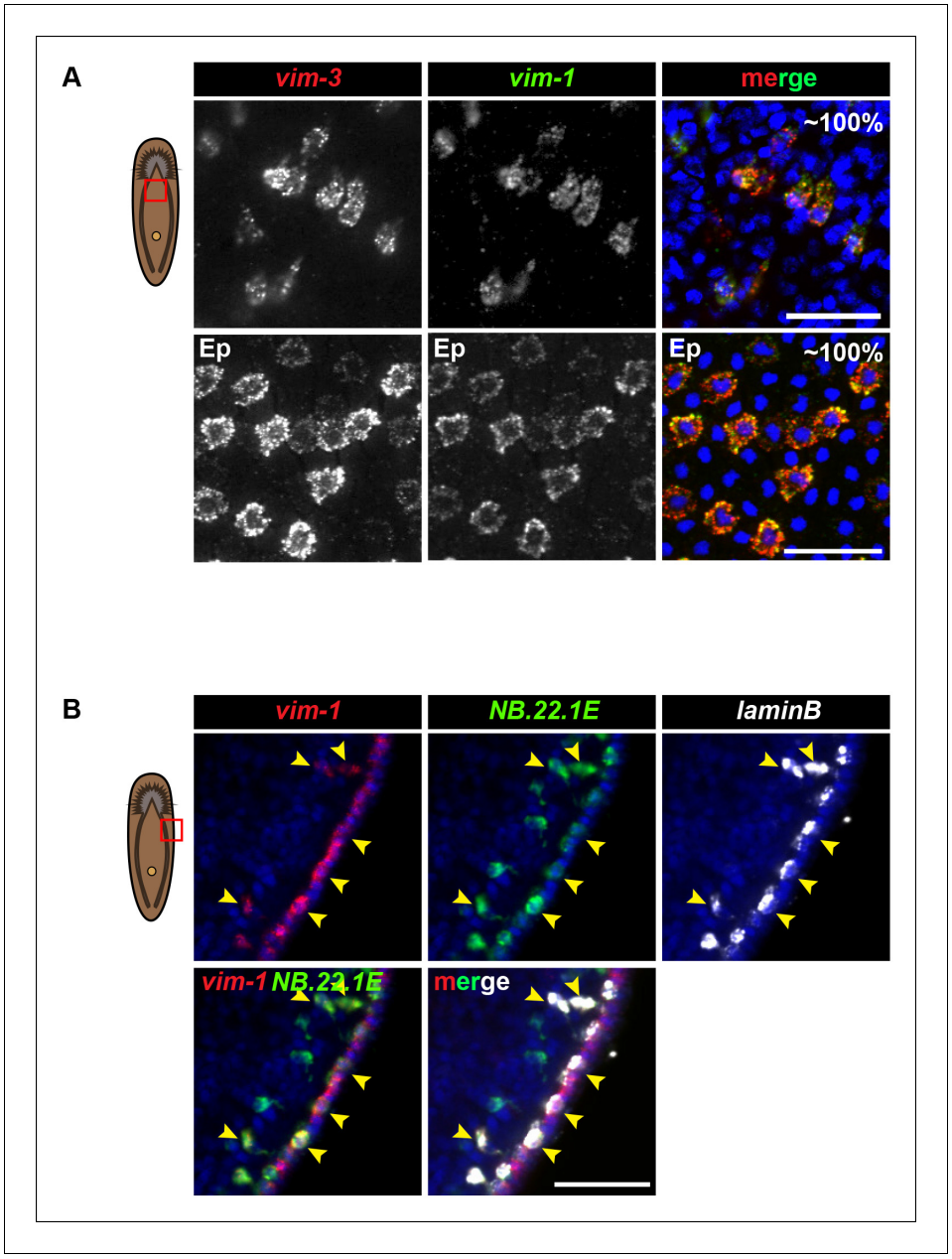

Figure 4—figure supplement 1. *Vim-3* and *vim-1* are co-expressed in the same cell types. (**A**) Images represent single confocal planes from ventral anterior regions of the mesenchyme (top panels) and epidermis (Ep) (bottom panels). Percentages represent fraction of *vim-3*$^{+}$ cells that co-express *vim-1* (~200 mesenchymal cells and 400 epidermal cells were quantified). Scale bars: 50 μm. (**B**) *Vim-1/vim-3* is expressed in *NB.22.1E*$^{+}$ and *laminB*$^{+}$ cells at the animal body margin (yellow arrowheads). Images represent single confocal planes. Scale bar: 50 μm.
DOI: http://dx.doi.org/10.7554/eLife.10501.013

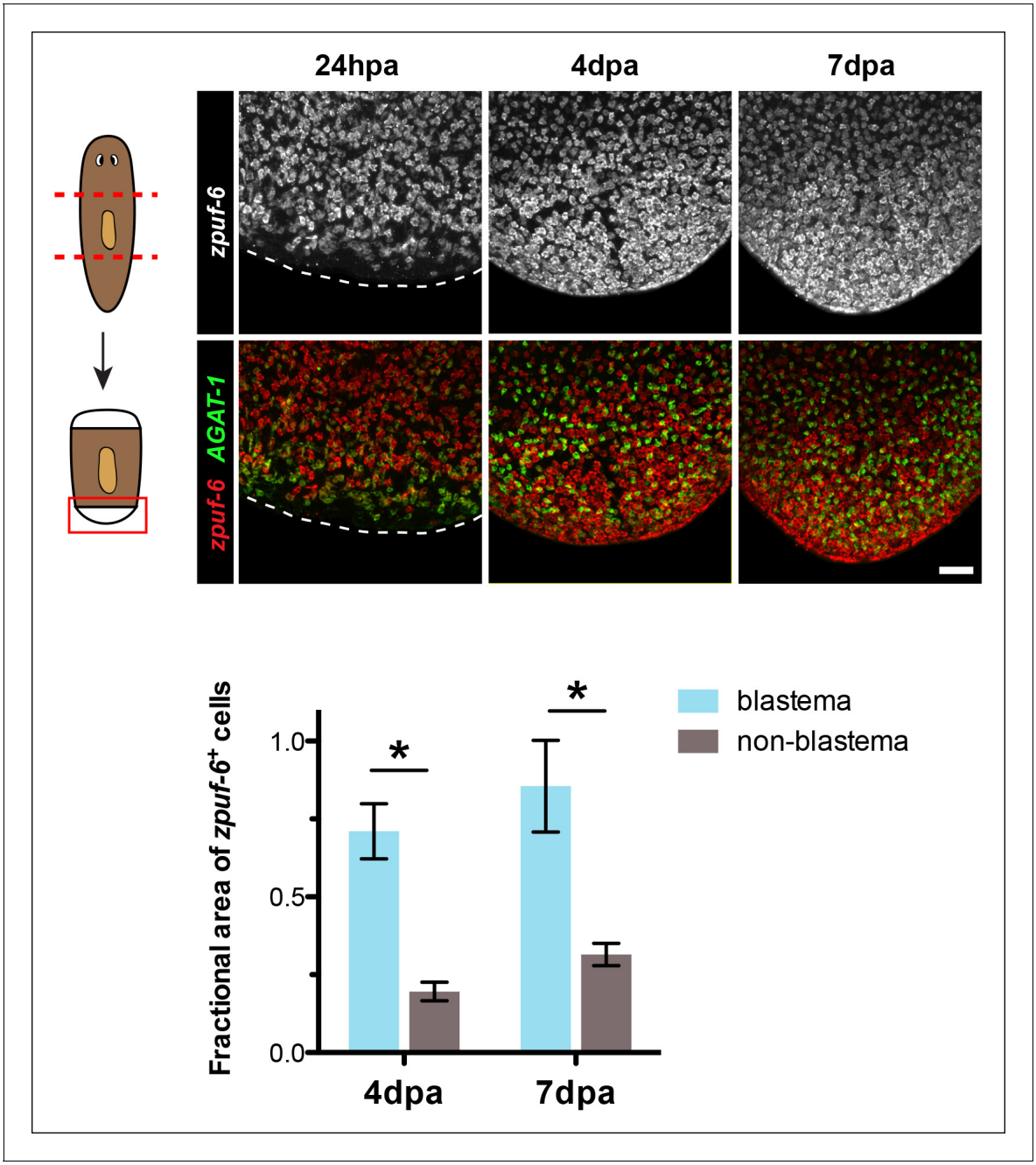

Figure 4—figure supplement 2. *zpuf-6*$^{+}$ cells are enriched at regenerating blastemas. Shown are posterior trunk fragments cut from wild-type animals and regenerated for the indicated times: hours or days post-amputation (hpa and dpa, respectively) and subjected to double FISH with *zpuf-6* and *AGAT-1*. Dotted lines demarcate the posterior end of the animal. Maximum intensity projections are shown. Scale bar: 100 μm. Quantification of the fractional area of *zpuf-6*$^{+}$ cells in the regenerating blastema compared to non-blastema (old tissue). The overall positive signal of *zpuf-6*$^{+}$ cells was measured in a fixed region in the blastema compared to the same area in the non-blastema region. Data represent means from 2 regenerating trunk fragments for each time point; error bars: SD. Student's t test: *, $p < 0.05$.

DOI: http://dx.doi.org/10.7554/eLife.10501.014

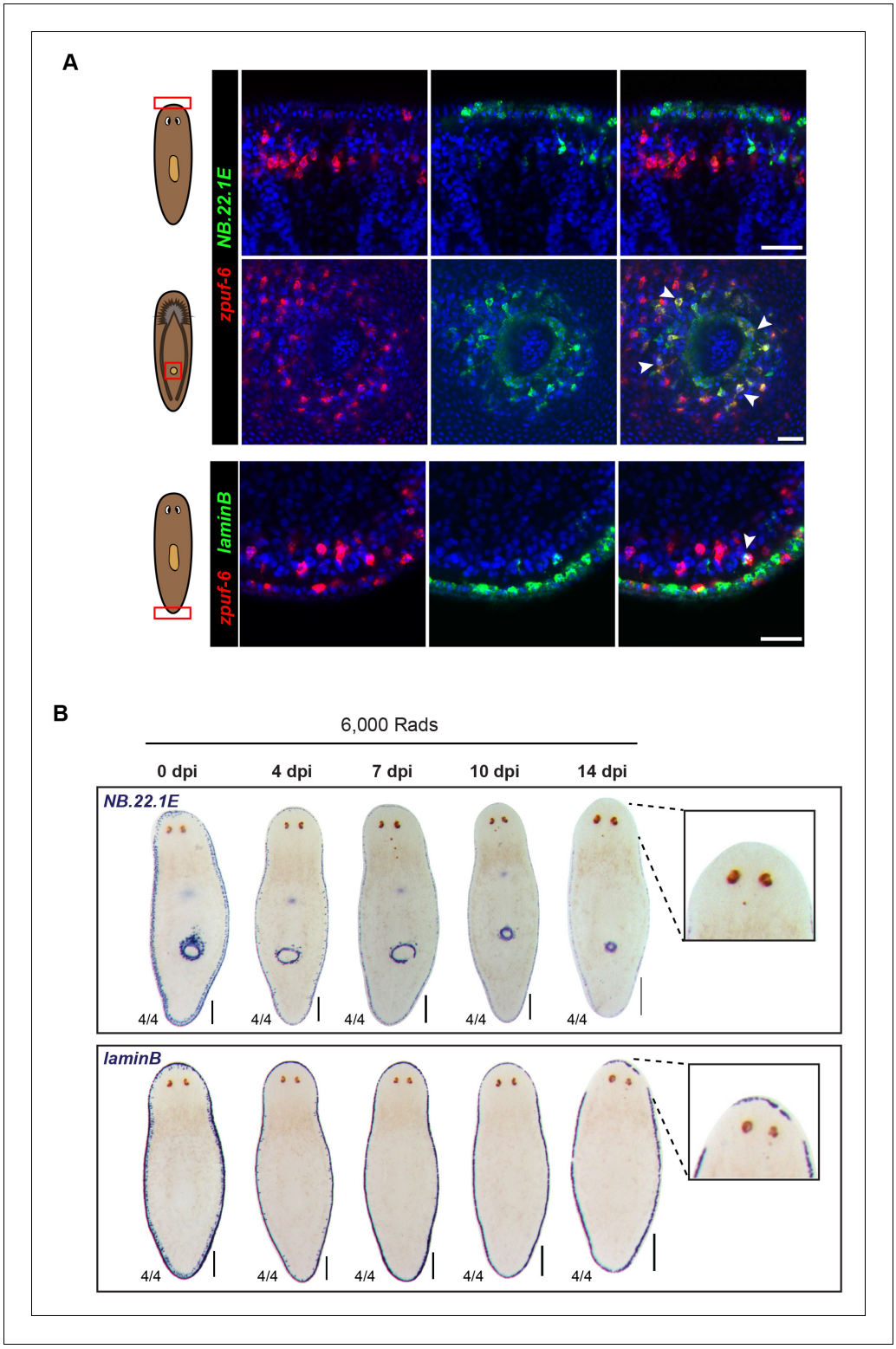

Figure 4—figure supplement 3. *NB.22.1E*$^{+}$ and *laminB*$^{+}$ cells exhibit little overlap with *zpuf-6* and display slow cell turnover kinetics after irradiation. (**A**) Whole-mount FISH of *zpuf-6* and markers of epidermal edge cells (*NB.22.1E* and *laminB*). *zpuf-6* exhibits little to no overlap with *NB.22.1E* in edge cells (top row) but overlaps with *NB.22.1E*$^{+}$ epidermal cells surrounding the ventral mouth opening (middle row, white arrowheads). *zpuf-6* shows very little overlap with *laminB*$^{+}$ edge cells (bottom row, white arrowheads). Scale bars: 50 μm. (**B**) Colorimetric WISH of animals after 6,000 Rad irradiation exposure for markers *NB.22.1E* and *laminB*. By 14dpi (days post-

Figure 4—figure supplement 3. continued on next page

Figure 4—figure supplement 3. Continued

irradiation), cells around the anterior have disappeared, suggesting that these cells do not turnover as quickly as *zpuf-6*$^{+}$ epidermal cells. For *NB.22.1E* marker, sub-epithelial mesenchymal cells and those around the ventral mouth opening disappear by 7dpi, suggesting they turn over more rapidly than the cells at animal margin. Ventral views. Scale bars: 200 μm.

DOI: http://dx.doi.org/10.7554/eLife.10501.015

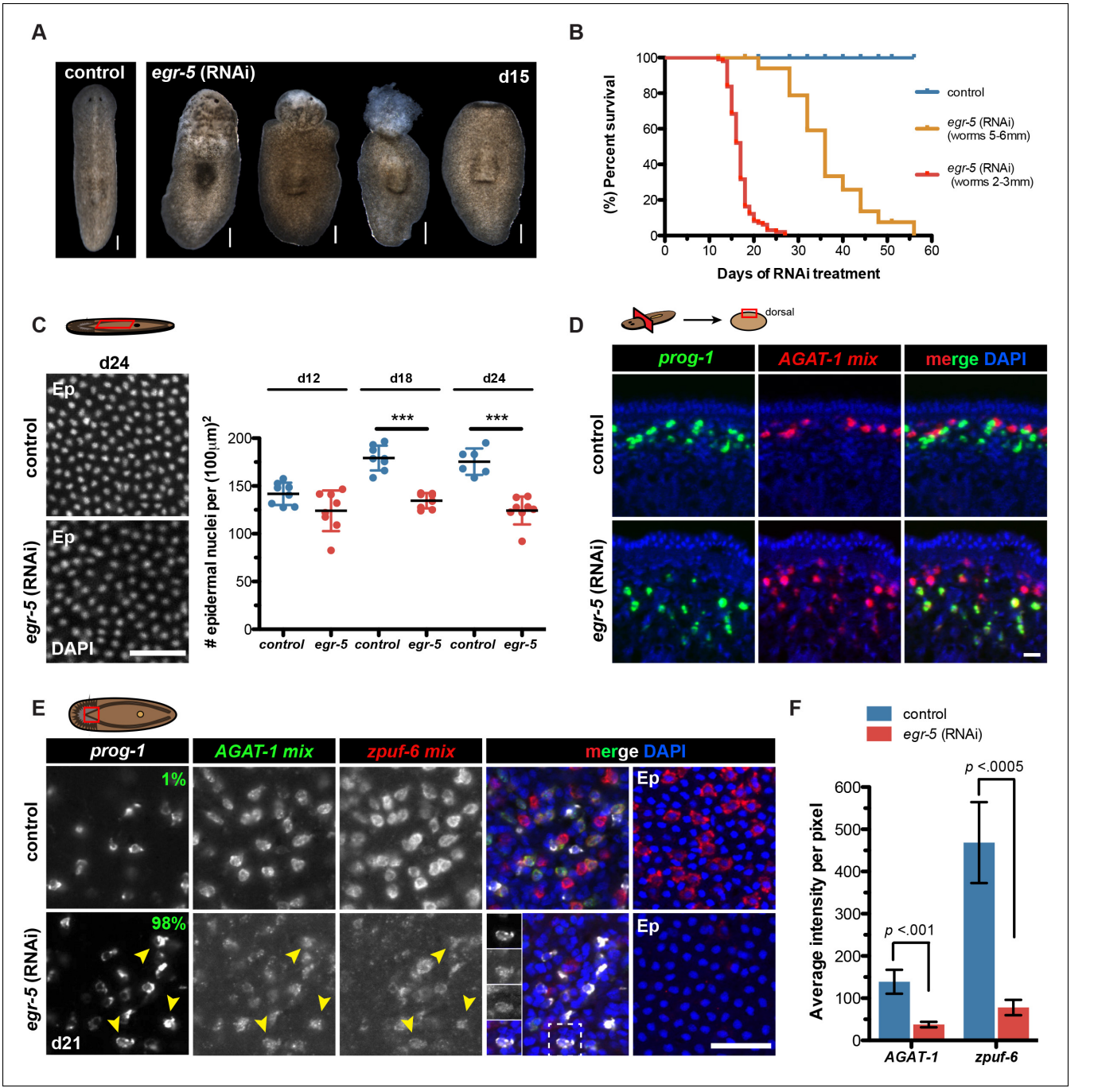

Figure 5. *Egr-5* is required for the proper differentiation of epidermal progeny cells. (**A**) Intact phenotypes for representative control and *egr-5*(RNAi) animals. Various stages of phenotypic progression of *egr-5* RNAi knockdown (4Fd15) are shown. Scale bars: 200 µm. (**B**) Survival curves for control and *egr-5*(RNAi) animals. The efficacy of RNAi and resulting gross phenotype is dependent on size of animals at the start of RNAi feedings. Animals starting around 2-3 mm in size (red lines) were fed 5 times (5F) (n = 99); animals starting around 5-6 mm in size (yellow lines) were fed 6 times (6F) (n = 65). Death was marked by complete animal lysis. (**C**) Effects of *egr-5*(RNAi) on epidermal cell density. DapI was used to quantify epidermal (Ep) nuclear density in the ventral mid-sections; representative images for 4Fd24 are shown. Scale bar: 50 µm. Quantification of epidermal cell density are plotted for d12, d18 and d24 for control (blue) and *egr-5*(RNAi) (red) animals. Each symbol represents individual animals (average of 2 regions/animal). Black lines and error bars (colored) represent mean and SD, respectively. Student's t test: ***, p <0.00005. (**D**) Spatial domain expansion of *prog-1* and *AGAT-1* cells in *egr-5*(RNAi). Tissue transverse sections of control and *egr-5*(RNAi) animals stained for markers of early epidermal progeny cells (8Fd30). To help improve visualization of *AGAT-1*-expressing cells, an RNA probe mix of other *AGAT-1* co-expressed genes were used (*AGAT-1* mix = *AGAT-1*,

Figure 5. continued on next page

Figure 5. Continued

zpuf-1, *zpuf-3*, *zpuf-4*). Scale bar: 10 μm. (**E**) Misexpression of epidermal progeny markers in *egr-5*(RNAi) animals. Triple FISH of *prog-1*, *AGAT-1* and *zpuf-6* markers in control and *egr-5*(RNAi) animals (4Fd21). Percentages shown in *prog-1* panel represent percentage of *prog-1*$^{+}$ cells that also express *AGAT-1* (400–700 cells were counted between 3–4 worms per condition). Yellow arrowheads highlight cells that are *prog-1*$^{+}$ *AGAT-1*$^{+}$ *zpuf-6*$^{+}$ (also shown in inset panels in merge panel). Rightmost column: epidermal (Ep) view highlighting loss of *zpuf-6* expression in epidermis. *AGAT-1* mix = *AGAT-1*, *zpuf-1*, *zpuf-3*, *zpuf-4; zpuf-6* mix = *zpuf-6*, *zpuf-5* and *zpuf-8*. Scale bar: 50 μm. (**F**) Average fluorescence intensity for *AGAT-1* mix and *zpuf-6* mix probes in control and *egr-5*(RNAi) animals from (**E**). Error bars: SD. p-values are results of unpaired Student's t test.

DOI: http://dx.doi.org/10.7554/eLife.10501.016

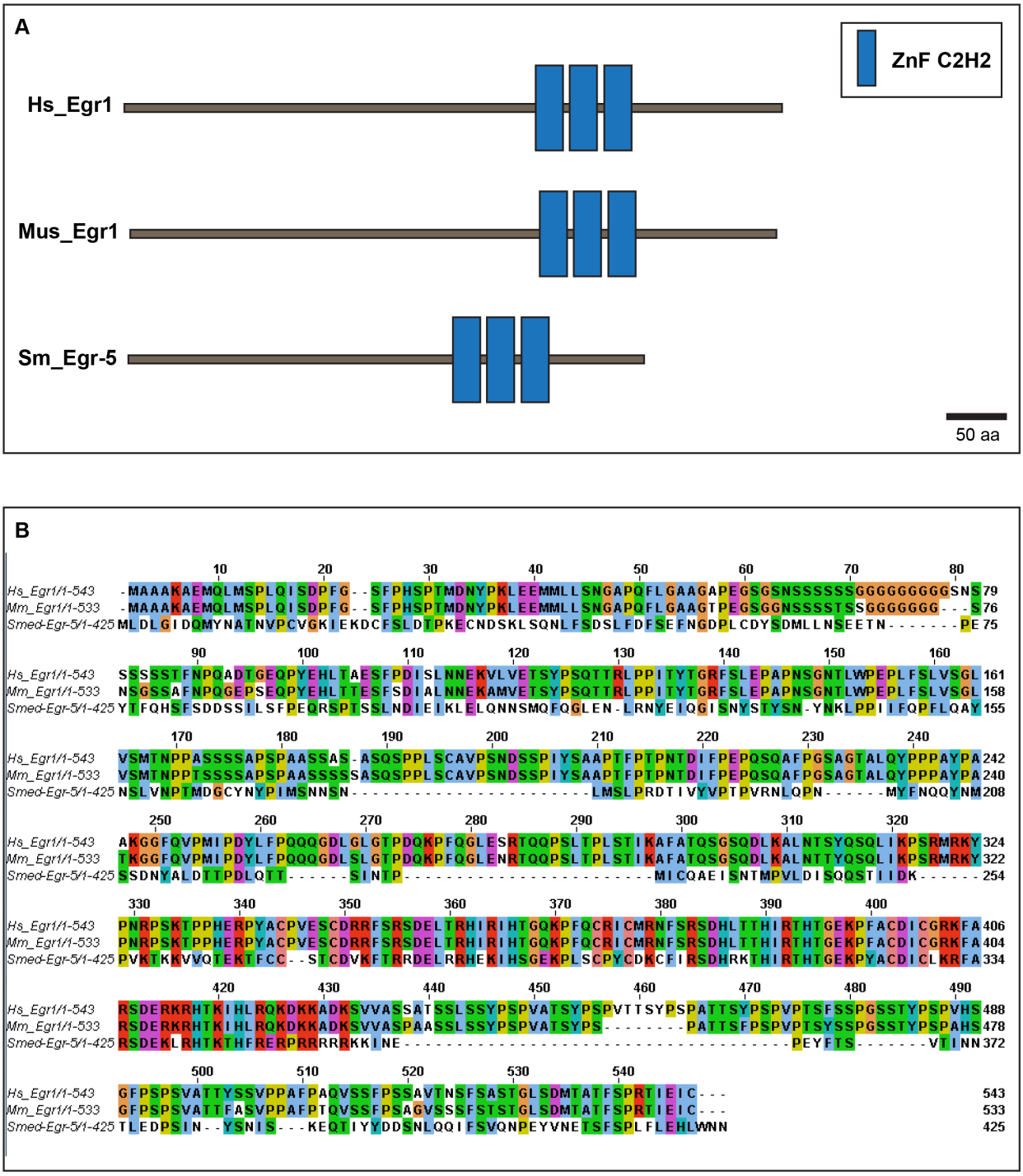

Figure 5—figure supplement 1. Smed-Egr-5 is a conserved member of the early growth response family of transcription factors. (**A**) Schematic of predicted domain structures of Smed-Egr-5 (Sm) with Egr1 from humans (Hs) and mouse (Mus), adapted from the Smart Modular Architecture Research Tool (SMART) (http://smart.embl-heidelberg.de).(**B**) Alignment of planarian Egr-5 protein sequence (Smed-Egr-5) with Egr1 sequences from human (Hs) and *Mus musculus* (Mm). Predicted Sm ZnF_C2H2 domains are residues 268-346.

DOI: http://dx.doi.org/10.7554/eLife.10501.017

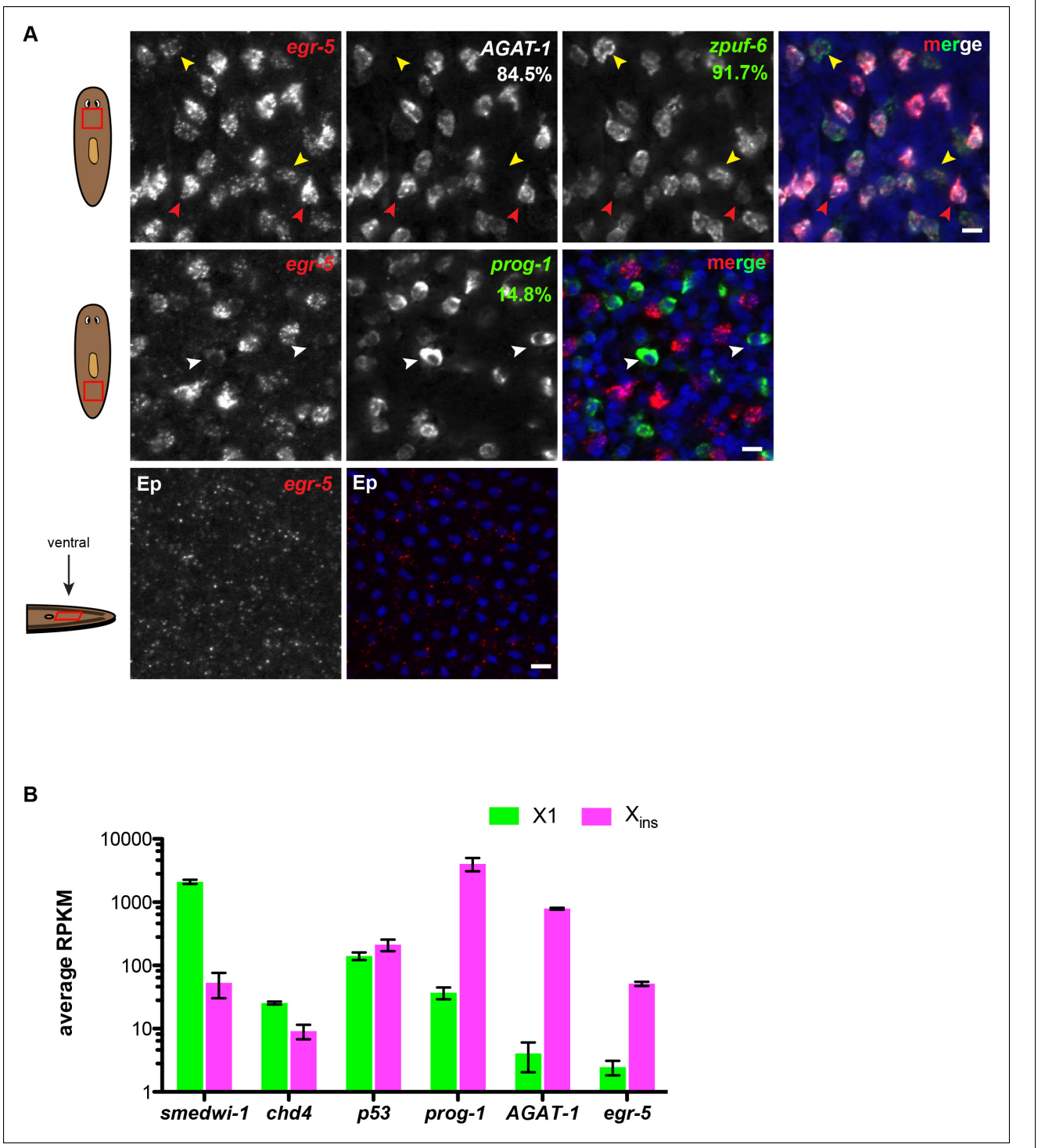

Figure 5—figure supplement 2. *Egr-5* is expressed in multiple post-mitotic epidermal progeny cells. (**A**) Whole-mount FISH of *egr-5* with various markers in the epidermal lineage. Top panel: Cells expressing the strongest levels of *egr-5* exhibit strong *AGAT-1* expression and very weak *zpuf-6* expression (red arrowheads). Cells expressing lower levels of *egr-5* exhibit strong *zpuf-6* expression and little to no detectable *AGAT-1* expression (yellow arrowheads). Middle panel: Some cells expressing low levels of *egr-5* are *prog-1*$^{+}$ (white arrowheads). Bottom panel: *egr-5* is very weakly expressed in some epidermal cells, which overlap with *zpuf-6*$^{+}$ epidermal cells (not shown). Percentages represent fraction of *egr-5*$^{+}$ cells (low but detectable expression was counted) that co-express the candidate gene (~~200-400 cells were quantified). Images are single confocal planes. Ep, epidermis. Scale bars: 10 μm. (**B**) *egr-5* transcripts are enriched in the post-mitotic, differentiated cell population (Xins). Average RPKM values are

Figure 5—figure supplement 2. continued on next page

Figure 5—figure supplement 2. Continued

plotted for various known neoblast and non-neoblast genes from wild-type planarian cells dissociated by FACS (data are deposited under GEO accession number: GSE73027). X1 cells are irradiation-sensitive and comprise of genes that are expressed in stem cells (*smedwi-1*). Xins cells are irradiation-insensitive and represent a population of various post-mitotic cells. *chd4* and *p53* are expressed in both stem cells and post-mitotic cells and are therefore present in both X1 and Xins cell population. *prog-1* and *AGAT-1* are post-mitotic epidermal lineage markers and show enrichment in the Xins population. *egr-5* has no detectable expression in stem cells based on FISH (not shown), and consistent with this, few *egr-5* transcripts are detected in the X1 population.

DOI: http://dx.doi.org/10.7554/eLife.10501.018

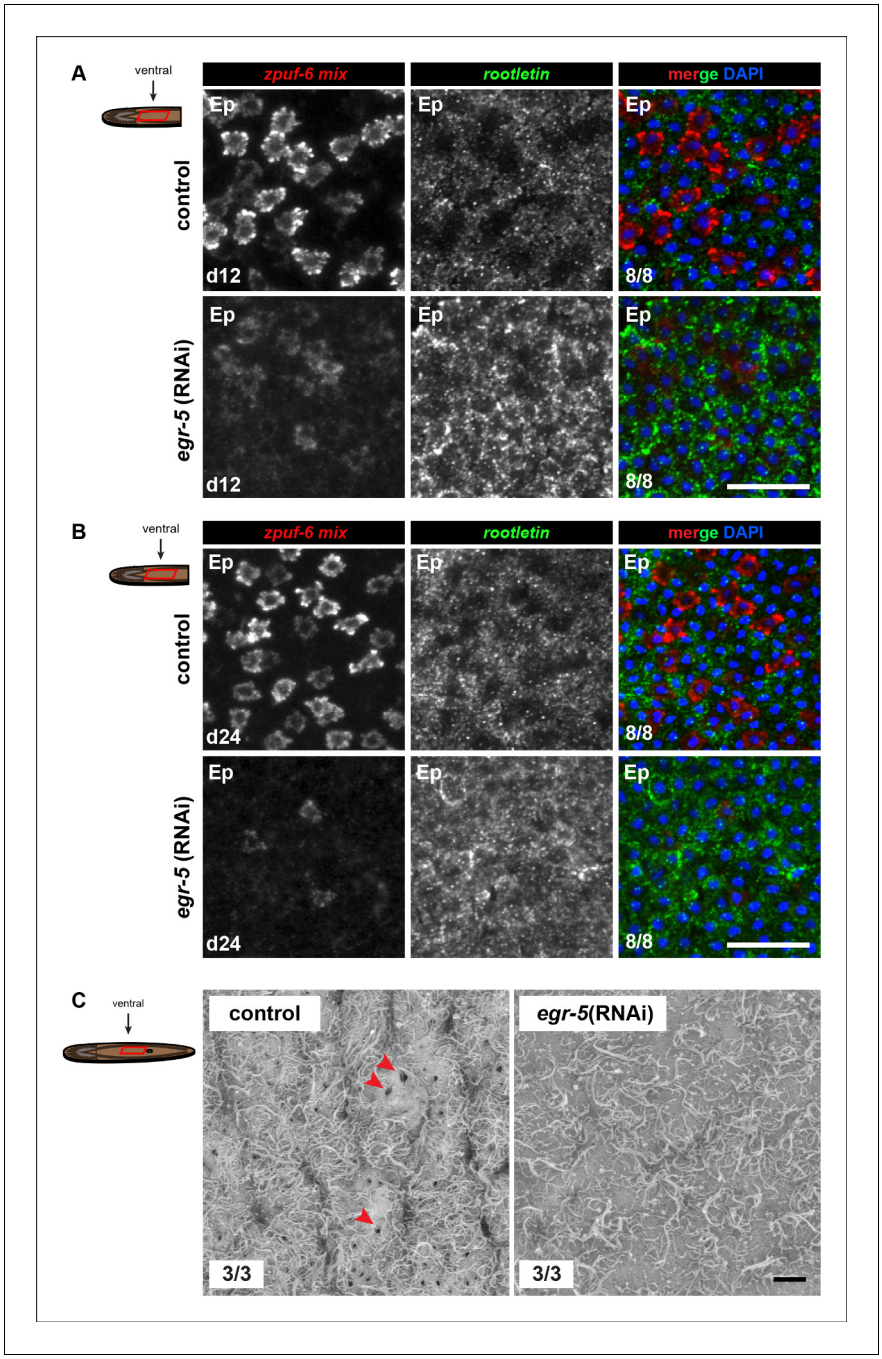

Figure 5—figure supplement 3. Molecular and ultrastructural analysis of *egr-5*(RNAi) epidermis. (**A**,**B**) Expression patterns of *zpuf-6* and *rootletin* cilia gene marker at (A) 4Fd12 and (B) 4Fd24 after initial RNAi treatment for control and *egr-5*(RNAi) animals. Representative images are single confocal planes of ventral epidermis (Ep). Scale bars: 50 μm. (**C**) Scanning electron micrograph of images (1500X) of control and *egr-5*(RNAi) animals (4Fd12) of the ventral epidermis (Ep) right above the mouth opening. Although cilia are still present in *egr-5*(RNAi) animals, there is an absence of epidermal pores (red arrowheads) that may be a result of epithelial stretching. Scale bar: 10 μm.
DOI: http://dx.doi.org/10.7554/eLife.10501.019

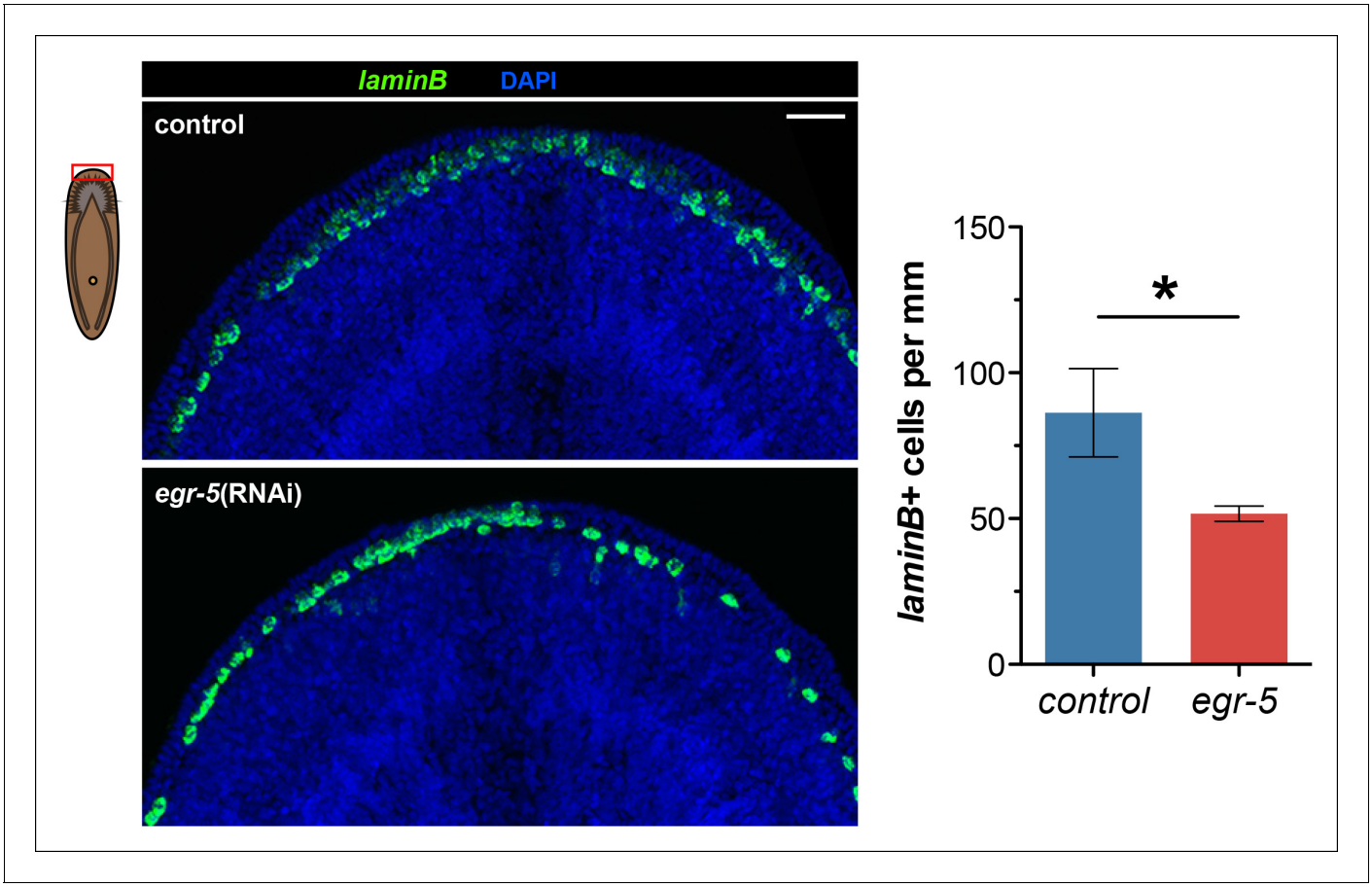

Figure 5—figure supplement 4. Reduction of *laminB*$^{+}$ cells in *egr-5*(RNAi) animals. The number of *laminB*$^{+}$ cells per mm along the animal margin was quantified in control and *egr-5*(RNAi) animals. The quantified region was restricted to the anterior because this region exhibits the highest cell turnover of *laminB*$^{+}$ cells. Representative images for 4Fd21 are shown. Scale bar: 50 μm. Quantification of *laminB*$^{+}$ cell density is plotted from 3 animals for each condition. Data represent means; error bars: SD. Student's t test: *, $p < 0.05$.

DOI: http://dx.doi.org/10.7554/eLife.10501.020

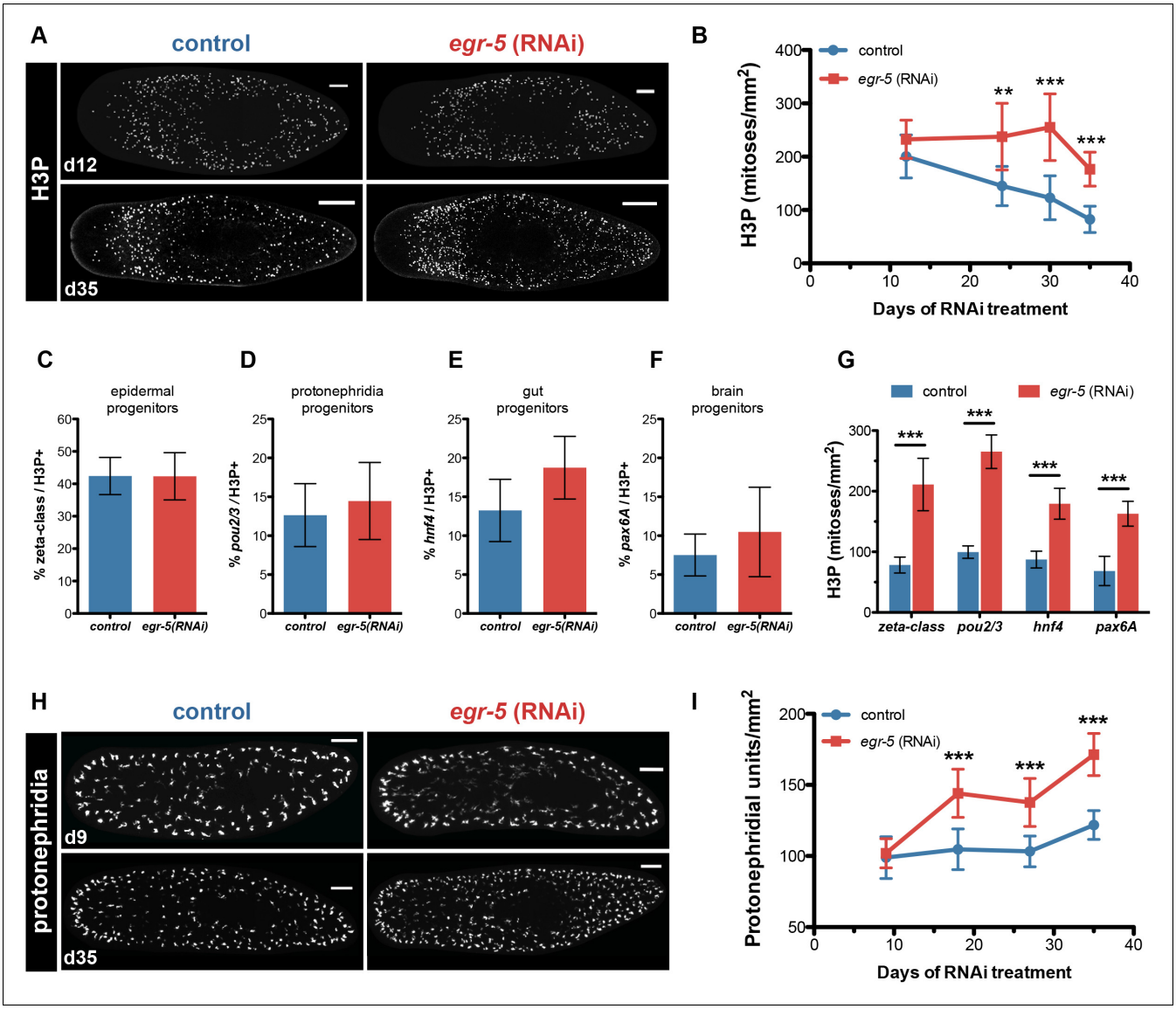

Figure 6. *Egr-5* knockdown results in the expansion of multiple progenitor populations. (**A**,**B**) *egr-5* knockdown causes an increase in global stem cell proliferation. (**A**) H3P-positive cells over the surface area in control and *egr-5*(RNAi) intact animals (8 feedings). Maximum intensity projections of representative H3P patterns for day 12 and day 35 time points are shown. Scale bar: 200 μm. (**B**) Quantification of H3P-positive cells per surface area from (A). Data represent means, error bars: SD. Student's t test: **, p <0.005, ***, p <0.0001. (**C**–**G**) Stem cell proliferation results in the expansion of multiple lineage-committed progenitors. For control and *egr-5*(RNAi) animals (3Fd27), animals were fixed and stained for H3P and a marker for the following: (**C**) dividing epithelial progenitors (zeta class: *zfp-1, egr-1, fgfr-1*), (**D**) dividing protonephridia progenitors (*pou2/3*), (**E**) dividing gut progenitors (*hnf4*), and (**F**) dividing brain progenitors (*pax6A*). Quantifications of percentage of lineage-committed progenitors of total $H3P^+$ cells are shown. Error bars: SD. (**G**) Quantification of total mitotic cells (H3P) per surface area for control and *egr-5*(RNAi) animals (3Fd27) from analysis in (**C**–**F**). Data represent means, error bars: SD. Student's t test: ***, p <0.0001. (**H**,**I**) *egr-5* knockdown causes supernumerary protonephridial units (PU). (**H**) Control and *egr-5*(RNAi) intact animals (8 feedings) were stained for the number of proximal units (*slc6a-13*) to visualize and quantify total PUs. Maximum intensity projections of representative animals for day 9 and day 35 time points are shown. Scale bar: 200 μm. (**I**) Quantification of PU per surface area. Data represent means, error bars: SD. Student's t test: ***, p <0.0001.

DOI: http://dx.doi.org/10.7554/eLife.10501.021

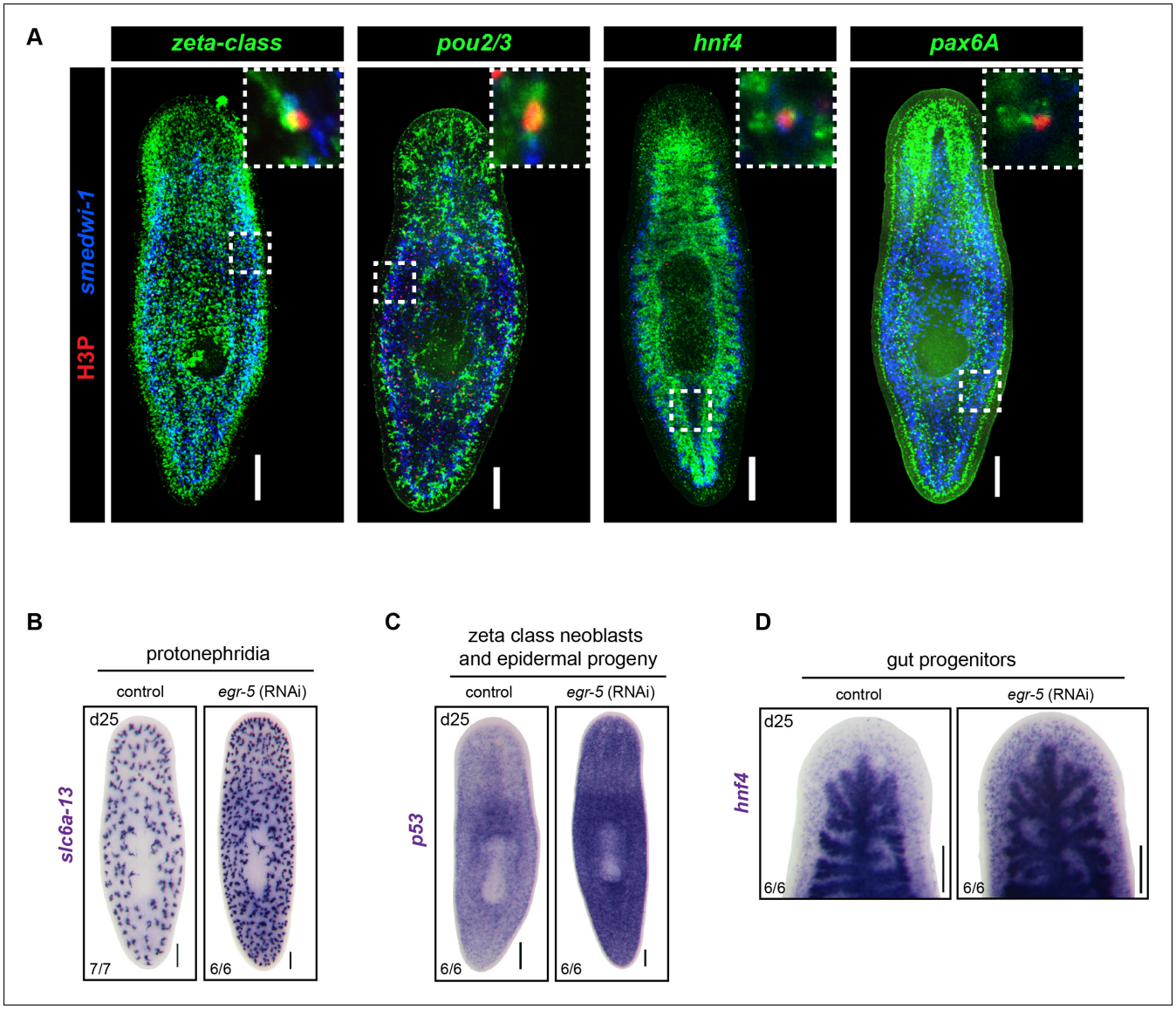

Figure 6—figure supplement 1. Analysis of multiple dividing tissue progenitors in *egr-5*(RNAi) animals. (**A**) Representative images of *egr-5*(RNAi) animals from ***Figure 6C–G*** fixed and stained for H3P (red), neoblast marker (blue: *smedwi-1*) and progenitor marker (green). Progenitor markers: zeta-class/epidermal: *zfp-1*, *egr-1*, *fgfr-1*; protonephridia: *pou2/3*; gut: *hnf4*; brain: *pax6A*. Images represent whole-animal maximum intensity projections and zoomed image highlights an example of a positive dividing progenitor cell (i.e. $H3P^{+}$/*smedwi-1*$^{+}$/progenitor marker^{+}). Scale bars: 200 μm. (**B-D**) Expansion of multiple differentiated tissue markers in *egr-5*(RNAi) animals. Representative colorimetric WISH images of control and *egr-5*(RNAi) intact animals (6Fd25) monitoring various lineages/tissues: protonephridia (*pou2/3*), epidermal progenitors and early/late progeny cells (*p53*), and gut morphology/gut progenitors (*hnf4*). Scale bars: 200 μm.

DOI: http://dx.doi.org/10.7554/eLife.10501.022

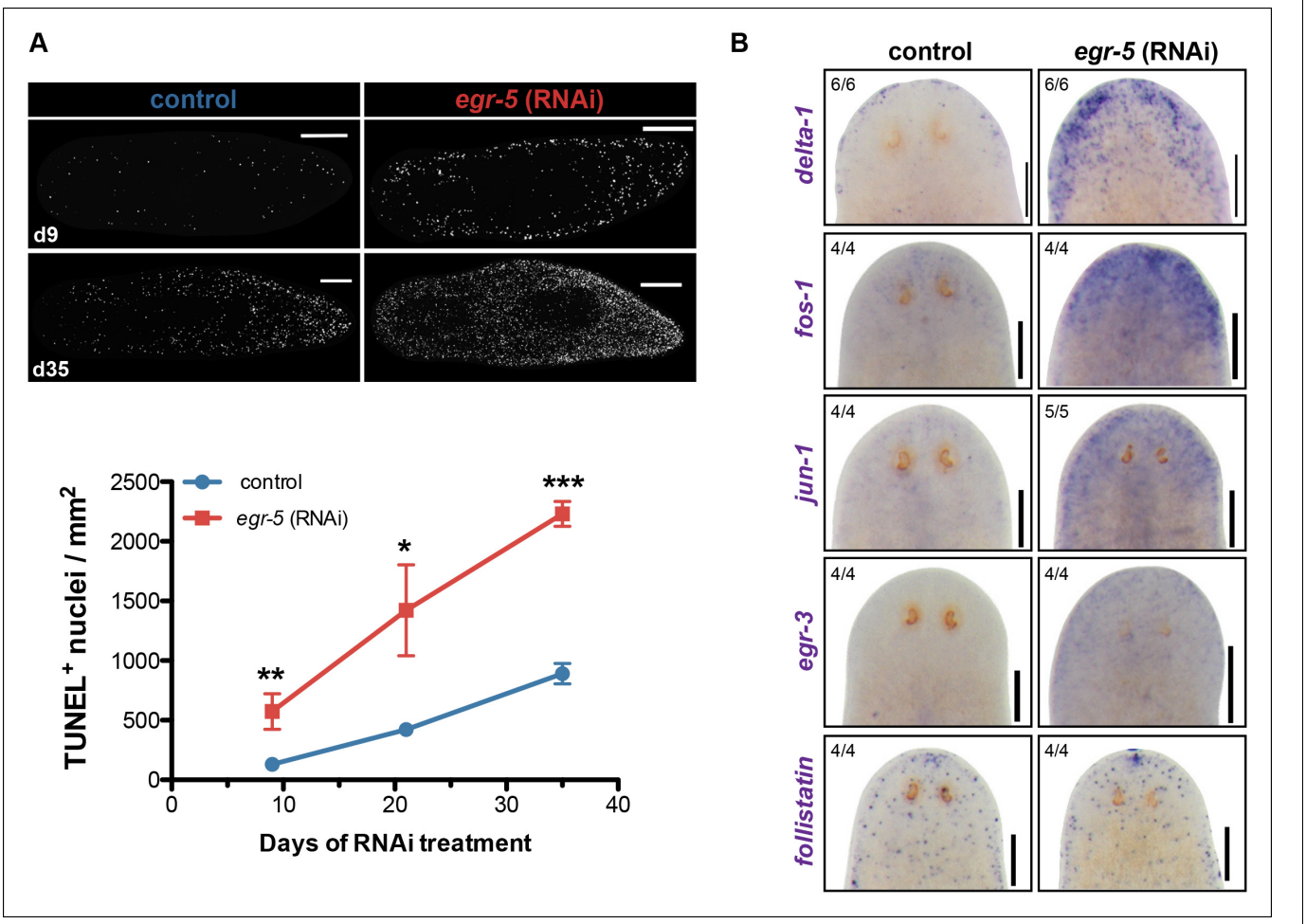

Figure 7. A global stress response is induced by loss of *egr-5*. (**A**) Whole-mount TUNEL assay measuring apoptosis in control and *egr-5*(RNAi) animals (8 feedings). Quantification of TUNEL-positive nuclei per surface area is plotted. Data represent means; error bars: SEM. Student's t test: *, p <.05, **, p <.005, ***, p <.0001. Representative maximum intensity projection of TUNEL-stained image for day 9 and day 35 are shown. Scale bars: 200 μm. (**B**) Wound-induced genes are up-regulated in *egr-5*(RNAi) animals. Representative colorimetric WISH images of *delta-1, fos-1, jun-1 egr-3 and follistatin* expression in the anterior regions of intact control and *egr-5*(RNAi) animals at 4Fd21 of RNAi treatment. Scale bars: 200 μm.

DOI: http://dx.doi.org/10.7554/eLife.10501.023

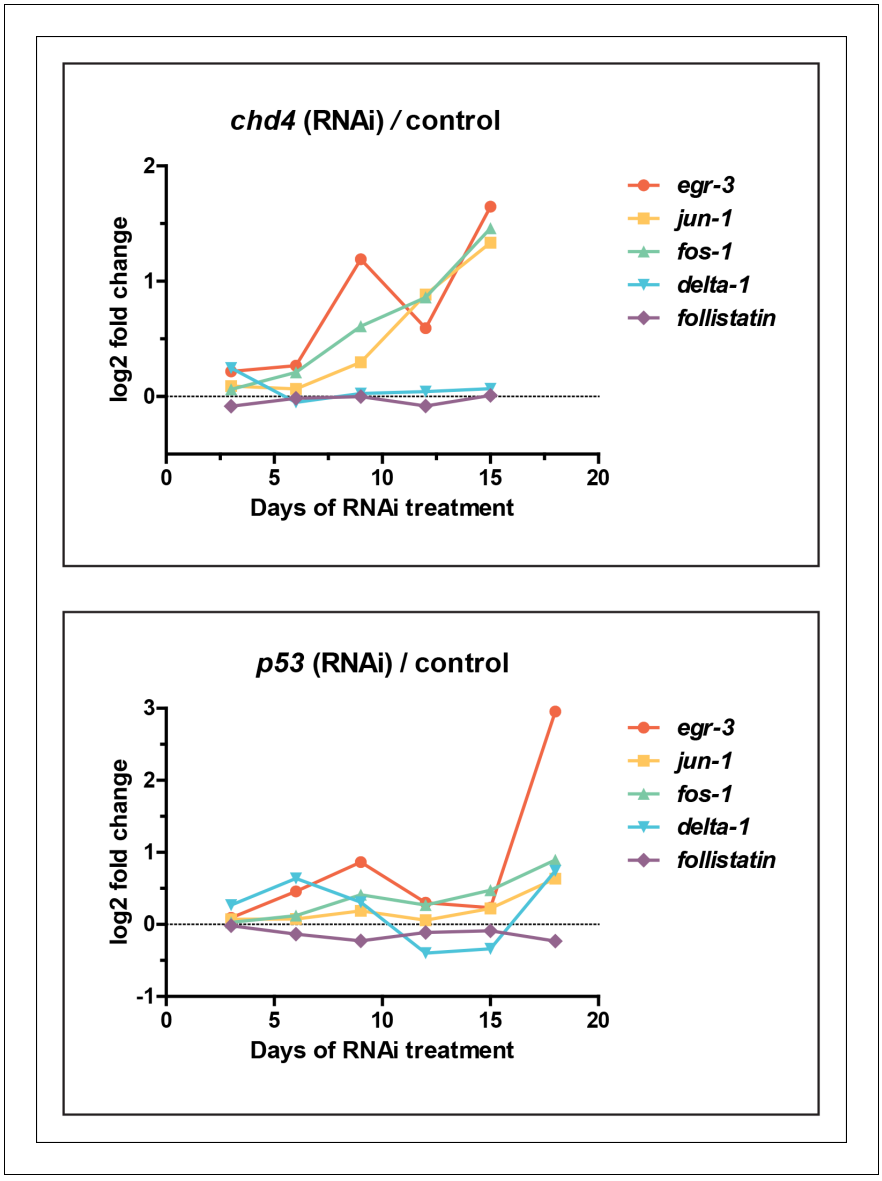

Figure 7—figure supplement 1. Wound-induced genes are upregulated in *chd4* and *p53* RNAi datasets. Plot of log2 ratios of selected wound-induced genes from ***Figure 7B*** in *chd4*(RNAi) (top panel) and *p53*(RNAi) (bottom panel) whole worm RNA-seq time course.

DOI: http://dx.doi.org/10.7554/eLife.10501.024

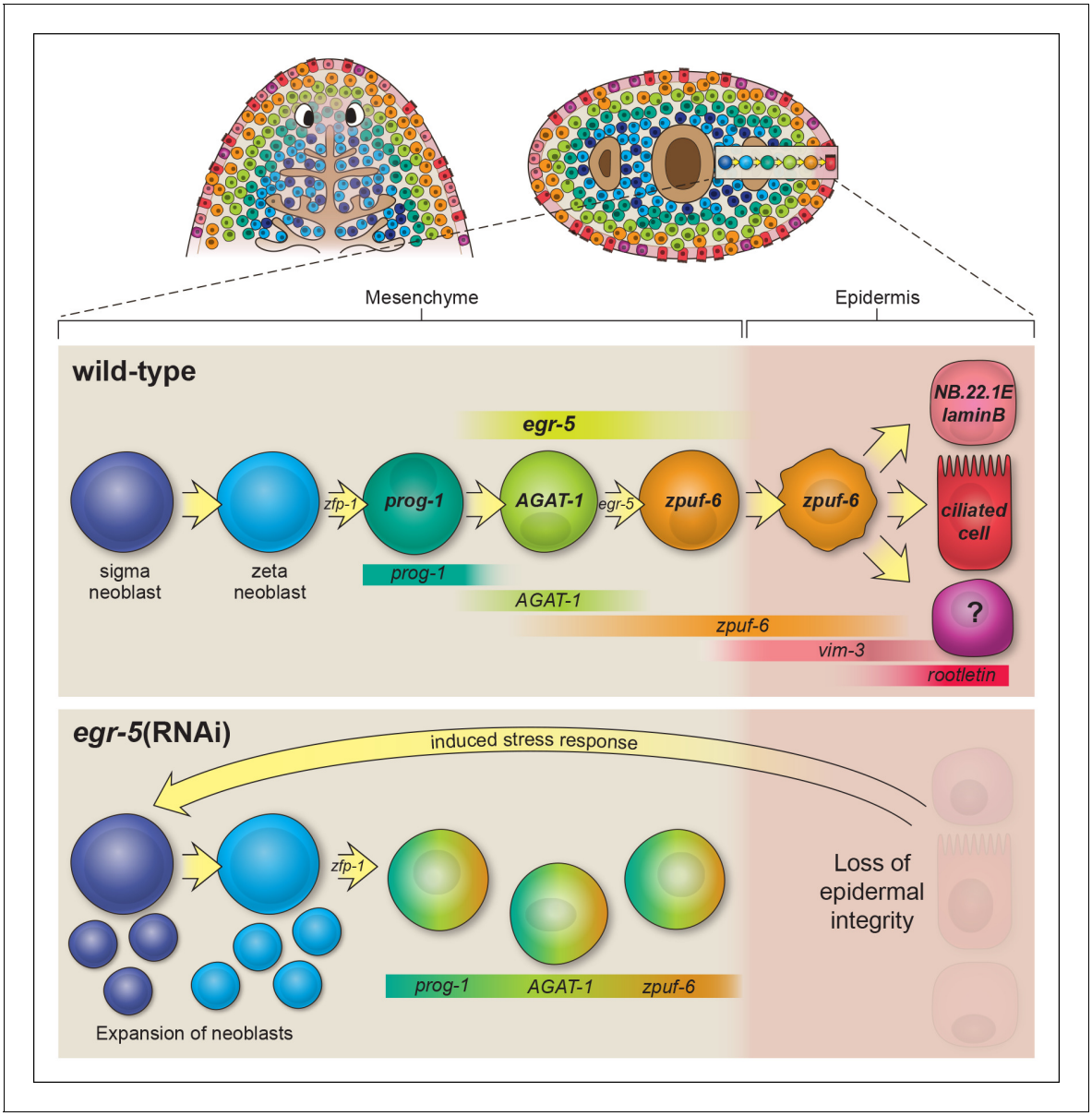

Figure 8. Model of planarian epidermal lineage progression. Schematic representation of the distribution of neoblasts, epidermal progeny cells in the mesenchyme, and differentiated epidermal cells along the anteroposterior (top left, dorsal view) and dorsoventral (top right, cross section) axes. Gut branches are shown as reference. Below: sigma-class neoblasts give rise to zeta-class neoblasts, which are epidermal progenitors. *zfp-1* is required to generate epidermal progeny cells, which begin to express different markers as cells undergo multiple transitions and intercalate into the mature epidermis. Gradient boxes represent domains and relative expression intensity of specified genes. *egr-5* is most strongly expressed in *AGAT-1*$^{+}$ cells and is required for proper differentiation of epidermal post-mitotic progeny cells. *zpuf-6*$^{+}$ epidermal cells likely represent a branching point in the epidermal cell fate decision and can generate multiple different cell types including marginal adhesive cells (*NB.22.1E* and *laminB*), multiciliated cells (*rootletin*), and other unknown cell types. Bottom panel: schematic of *egr-5*(RNAi) phenotype. Loss of *egr-5* disrupts the proper spatiotemporal transition of post-mitotic epidermal cells, resulting in *prog-1*, *AGAT-1* and *zpuf-6* to be co-expressed in the same cell, and leading to a depletion of mature epidermal cells. The resulting loss of epidermal integrity is sensed by the neoblasts (induced stress response) and causes an expansion of neoblasts and multiple progenitors before animals eventually lyse due to irreparable loss of an intact epidermal barrier.

DOI: http://dx.doi.org/10.7554/eLife.10501.025